NUREG/CR-1171
HEDL-TME 79-65
R5, RF

THE EFFECT OF CRACK LENGTH AND SIDE GROOVES ON THE DUCTILE FRACTURE TOUGHNESS PROPERTIES OF ASTM A533 STEEL

Hanford Engineering Development Laboratory

HANFORD ENGINEERING DEVELOPMENT LABORATORY
Operated by Westinghouse Hanford Company
P.O. Box 1970 Richland, WA 99352
A Subsidiary of Westinghouse Electric Corporation
Prepared for the U.S. Nuclear Regulatory Commission
under Interagency Agreement DE-AC14-76FF02170
NRC FIN No. B0119

Available from

GPO Sales Program
Division of Technical Information and Document Control
U. S. Nuclear Regulatory Commission
Washington, D. C. 20555

and

National Technical Information Service
Springfield, Virginia 22161

NUREG/CR-1171
HEDL-TME 79-65
R5, RF

THE EFFECT OF CRACK LENGTH AND SIDE GROOVES ON THE DUCTILE FRACTURE TOUGHNESS PROPERTIES OF ASTM A533 STEEL

Hanford Engineering Development Laboratory

K.W. Carlson
J.A. Williams

January 1980

HANFORD ENGINEERING DEVELOPMENT LABORATORY
Operated by Westinghouse Hanford Company
P.O. Box 1970 Richland, WA 99352
A Subsidiary of Westinghouse Electric Corporation

Prepared for the
Division of Reactor Safety Research
Office of Nuclear Regulatory Research
U.S. Nuclear Regulatory Commission
Washington, D.C. 20555
NRC FIN No. B0119

NUREG/CR-1171
HEDL-TME 79-65
R5, RF

THE EFFECT OF CRACK LENGTH AND SIDE GROOVES ON THE DUCTILE FRACTURE TOUGHNESS PROPERTIES OF ASTM A533 STEEL

K. W. Carlson
J. A. Williams

ABSTRACT

The ductile fracture toughness, J_{Ic}, and tearing modulus, T, of ASTM A533, Grade B, Class 1 steel were evaluated by the unloading compliance method for determining J-R curves. These properties were measured for a matrix of 1T specimens in which the relative crack length, a/W, and the depth of side grooving were systematically varied to determine their individual effects. In addition, the applicability of an LVDT extensometer system was investigated for use in the unloading compliance method for J-R curve determination.

ACKNOWLEDGEMENTS

The authors would like to extend their thanks to G. C. Massie, Senior Technician, for his careful attention in conducting the tests reported herein.

Sincere appreciation is also extended to Mr. G. D. Whitman of Oak Ridge National Laboratory and program manager for the HSST Program for his patience and encouragement during this phase of the investigation.

CONTENTS

FIGURES

FIGURES (Cont'd)

TABLES

FOREWORD

The Heavy Section Steel Technology (HSST) Program is a United States Nuclear Regulatory Commission (NRC) sponsored effort coordinated by the Oak Ridge National Laboratory (ORNL) with G. D. Whitman as the HSST Program Manager.

The HSST work performed at HEDL is being conducted under Department of Energy Contract DE-AC14-76FF02170 through a technical service contract with ORNL (Purchase Order 11Y-50917V). Westinghouse Hanford Company technical representative is L. D. Blackburn.

This report is designated Heavy Section Steel Technology Program Technical Report No. 55. Prior reports in this series are:

Report No.

1 S. Yukawa, Evaluation of Periodic Proof Testing and Warm Prestressing Procedures for Nuclear Reactor Vessels, HSSTP-TR-1, General Electric Company, Schenectady, NY, July 1, 1969.

2 L. W. Loechel, The Effect of Section Size on the Transition Temperature in Steel, Martin Marietta Company, Denver, CO, 1969.

3 P. N. Randall, Gross Strain Measure of Fracture Toughness of Steels, HSSTP-TR-3, TWR Systems Group, Redondo Beach, CA, November 1, 1969.

4 C. Visser, S. E. Gabrielse and W. VanBuren, A Two-Dimensional Elastic-Plastic Analysis of Fracture Test Specimens, WCAP-7368, Westinghouse Electric Corporation, PWR Systems Division, Pittsburgh, PA, October 1969.

5 T. R. Mager, F. O. Thomas and W. S. Hazelton, Evaluation by Linear Elastic Fracture Mechanics of Radiation Damage to Pressure Vessel Steels, WCAP-7328, Revised, Westinghouse Electric Corporation, PWR Systems Division, Pittsburgh, PA, October 1969.

6 W. O. Shabbits, W. H. Pryle and E. T. Wessel, Heavy Section Fracture Toughness Properties of A 533 Grade B Class 1 Steel Plate and Submerged Arc Weldment, WCAP-7414, Westinghouse Electric Corporation, PWR Systems Division, Pittsburgh, PA, December 1969.

7 F. J. Loss, Dynamic Tear Test Investigations of the Fracture Toughness of Thick-Section Steel, NRL 7056, U.S. Naval Research Laboratory, Washington, DC, May 14, 1970.

8 P. B. Crosley and E. J. Ripling, Crack Arrest Fracture Toughness of A533 Grade B, Class 1 Pressure Vessel Steel, HSSTP-TR-8, Materials Research Laboratory, Inc., Glenwood, IL, March 1970.

Report No.

9 T. R. Mager, Post-Irradiation Testing of 2 T Compact Tension Specimens, WCAP-7561, Westinghouse Electric Corporation, PWR Systems Division, Pittsburgh, PA, August 1970.

10 T. R. Mager, Fracture Toughness Characterization Study of A533, Grade B, Class 1 Steel, WCAP-7578, Westinghouse Electric Corporation, PWR System Division, Pittsburgh, PA, October 1970.

11 T. R. Mager, Notch Preparation in Compact Tension Specimens, WCAP-7579, Westinghouse Electric Corporation, PWR Systems Division, Pittsburgh, PA, November 1970.

12 N. Levy and P. V. Marcal, Three-Dimensional Elastic-Plastic Stress and Strain Analysis for Fracture Mechanics, Phase I: Simple Flawed Specimens, HSSTP-TR-12, Brown University, Providence, RI, December 1970.

13 W. O. Shabbits, Dynamic Fracture Toughness Properties of Heavy Section A533 Grade B, Class 1 Steel Plate, WCAP-7623, Westinghouse Electric Corporation, PWR Systems Division, Pittsburgh, PA, December 1970.

14 P. N. Randall, Gross Strain Crack Tolerance of A533-B Steel, HSSTP-TR-14, TRW Systems Group, Redondo Beach, CA, May 1, 1971.

15 H. T. Corten and R. H. Sailors, Relationship Between Materials Fracture Toughness Using Fracture Mechanics and Transition Temperature Tests, T&AM Report No. 346, University of Illinois, Urbana, IL, August 1, 1971.

16 T. R. Magner and V. J. McLoughlin, The Effect of an Environment of High Temperature Primary Grade Nuclear Reactor Water and the Fatigue Crack Growth Characteristics of A533 Grade B, Class 1 Plate and Weldment Material, WCAP-7776, Westinghouse Electric Corporation, PWR Systems Division, Pittsburgh, PA, October 1971.

17 N. Levy and P. V. Marcal, Three-Dimensional Elastic-Plastic Stress and Strain Analysis for Fracture Mechanics, Phase II: Improved Modeling, HSSTP-TR-17, Brown University, Providence, RI, November 1971.

18 S. C. Grigory, Six-Inch-Thick Flawed Tensile Tests, First Technical Summary Report, Longitudinal Specimens 1 Through 7, HSSTP-TR-18, Southwest Research Institute, San Antonio, TX, June 1972.

19 P. N. Randall, Effects of Strain Gradients on the Gross Strain Crack Tolerance of A533-B Steel, HSSTP-TR-19, TRW Systems Group, Redondo Beach, CA, May 1, 1972.

Report No.

20 S. C. Grigory, Tests of Six-Inch-Thick Flawed Tensile Specimens, Second Technical Summary Report, Transverse Specimens Numbers 8 Through 10, Welded Specimens Numbers 11 Through 13, HSSTP-TR-20, Southwest Research Institute, San Antonio, TX, June 1972.

21 Lee A. James and John A. Williams, The Effect of Temperature and Neutron Irradiation upon the Fatigue-Crack Propagation Behavior of ASTM A533, Grade B, Class 1 Steel, HEDL-TME 72-132, Hanford Engineering Development Laboratory, Richland, WA, September 1972.

22 S. C. Grigory, Tests of Six-Inch-Thick Flawed Tensile Specimens, Third Technical Summary Report, Longitudinal Specimens Numbers 14 Through 16, Unflawed Specimen Number 17, HSSTP-TR-22, Southwest Research Institute, San Antonio, TX, October 1972.

23 S. C. Grigory, Tests of Six-Inch-Thick Flawed Tensile Specimens, Fourth Technical Summary Report, Tests of One-Inch Thick Flawed Tensile Specimens for Size Effect Evaluation, HSSTP-TR-23, Southwest Research Institute, San Antonio, TX, June 1973.

24 S. P. Ying and S. C. Grigory, Tests of Six-Inch-Thick Tensile Specimens, Fifth Technical Summary Report, Acoustic Emission Monitoring of One-Inch and Six-Inch-Thick Tensile Specimens, HSSTP-TR-24, Southwest Research Institute, San Antonio, TX, November 1972.

25 R. W. Derby, et al., Test of Six-Inch-Thick Pressure Vessels, Series 1: Intermediate Test Vessels V-1 and V-2, ORNL-4895, Oak Ridge National Laboratory, Oak Ridge, TN, February 1974.

26 W. J. Stelzman and R. G. Berggren, Radiation Strengthening and Embrittlement in Heavy Section Plates and Welds, ORNL-4871, Oak Ridge National Laboratory, Oak Ridge, TN, June 1973.

27 P. B. Crosley and E. J. Ripling, Crack Arrest in an Increasing K-Field, HSSTP-TR-27, Materials Research Laboratory, Glenwood, IL, January 1973.

28 P. V. Marcal, P. M. Stuart and R. S. Bettes, Elastic-Plastic Behavior of a Longitudinal Semi-Elliptical Crack in a Thick Pressure Vessel, HSSTP-TR-28, Brown University, Providence, RI, June 1973.

31 J. A. Williams, The Irradiation and Temperature Dependence of Tensile and Fracture Properties of ASTM A533, Grade B, Class 1 Steel Plate and Weldment, HEDL-TME 73-75, Hanford Engineering Development Laboratory, Richland, WA, August 1973.

Report No.

32 J. M. Steichen and J. A. Williams, High Strain Rate Tensile Properties of Irradiated ASTM A533 Grade B, Class 1 Pressure Vessel Steel, HEDL-SA 581, Hanford Engineering Development Laboratory, Richland, WA, July 1973.

33 P. C. Riccardella and J. L. Swedlow, A Combined Analytical-Experimental Fracture Study, WCAP-8224, Westinghouse Electric Corporation, PWR Systems Division, Pittsburgh, PA, October 1973.

34 R. J. Podlasek and R.J. Eiber, Investigation of Mode III Crack Extension in Reactor Piping. Final Report, HSSTP-TR-34, Battelle Columbus Laboratories, Columbus, OH, May 1974.

35 T. R. Mager, et al., Interim Report on the Effect of Low Frequencies on the Fatigue Crack Growth Characteristics of A533 Grade B, Class 1 Plate in an Environment of High-Temperature Primary Grade Nuclear Reactor Water, WCAP-8256, Westinghouse Electric Corporation, Pittsburgh, PA, December 1973.

36 J. A. Williams, The Irradiated Fracture Toughness of ASTM A533, Grade B, Class 1 Steel Measured with a Four-Inch-Thick Compact Tension Specimen, HEDL-TME 75-10, Hanford Engineering Development Laboratory, Richland, WA, January 1975.

37 R. H. Bryan et al., Test of Six-Inch-Thick Pressure Vessels, Series 2: Intermediate Test Vessels V-3, V-4, and V-6, ORNL-5059, Oak Ridge National Laboratory, Oak Ridge, TN, November 1975.

38 T. R. Mager, S. E. Yanichko and L. R. Singer, Fracture Toughness Characterization of HSST Intermediate Pressure Vessel Material, WCAP-8456, Westinghouse Electric Corporation, Pittsburgh, PA, December 1974.

39 J. G. Merkle, G. D. Whitman and R.H. Bryan, An Evaluation of the HSST Program Intermediate Pressure Vessel Tests in Terms of Light-Water Reactor Pressure Vessel Safety, ORNL-TM-5090, Oak Ridge National Laboratory, Oak Ridge TN, November 1975.

40 J. G. Merkle et al., Test of Six-Inch-Thick Pressure Vessels, Series 3: Intermediate Test Vessel V-7, ORNL/NUREG-1, Oak Ridge National Laboratory, Oak Ridge, TN, August 1976.

41 J. A. Davidson, L. J. Ceschini, R. P. Shogan, and G. V. Rao, The Irradiated Dynamic Fracture Toughness of ASTM A533, Grade B, Class 1 Steel Plate and Submerged Arc Weldment, WCAP-8775, Westinghouse Electric Corporation, Pittsburgh, PA, October 1976.

Report No.

42 R. D. Cheverton, Pressure Vessel Fracture Studies Pertaining to a PWR LOCA-ECC Thermal Shock: Experiments TSE-1 and TSE-2, ORNL/NUREG-31, Oak Ridge National Laboratory, Oak Ridge, TN, September 1976.

43 P. P. Holz, J. G. Merkle, G. C. Robinson and J. E. Smith, Test of Six-Inch-Thick Pressure Vessels, Series 4: Intermediate Test Vessels V-5 and V-9, with Inside Nozzle Corner Cracks, ORNL/NUREG-7, Oak Ridge National Laboratory, Oak Ridge, TN, August 1977.

44 J. A. Williams, The Ductile Fracture Toughness of Heavy Section Steel Plate, NUREG/CR-0859, HEDL-TME 77-1, Hanford Engineering Development Laboratory, Richland, WA, September 1979.

45 R. H. Bryan, T. M. Cate, P. P. Holz, T. A. King, J. G. Merkle, G. C. Robinson, G. C. Smith, J. E. Smith and G. D. Whitman, Test of 6-In.-Thick Pressure Vessels. Series 3: Intermediate Test Vessel V-7A Under Sustained Loading, ORNL/NUREG-9, Oak Ridge National Laboratory, Oak Ridge, TN, February 1978.

46 R. D. Cheverton and S. E. Bolt, Pressure Vessel Fracture Studies Pertaining to a PWR LOCA-ECC Thermal Shock: Experiments TSE-3 and TSE-4 and Update of TSE-1 and TSE-2 Analysis, ORNL/NUREG-22, Oak Ridge National Laboratory, Oak Ridge, TN, December 1977.

47 D. A. Canonico, Significance of Reheat Cracks to the Integrity of Pressure Vessels for Light-Water Reactors, ORNL/NUREG-15, Oak Ridge National Laboratory, Oak Ridge, TN, July 1977.

48 G. C. Smity and P. P. Holz, Repair Weld Induced Residual Stresses in Thick-Walled Steel Pressure Vessels, NUREG/CR-0093 ORNL/NUREG/TM-153, Oak Ridge National Laboratory, Oak Ridge, TN, June 1978.

49 P. P. Holz and S. W. Wismer, Half-Bead (Temper) Repair Welding for HSST Vessels, NUREG/CR-0113 ORNL/NUREG/TM-177, Oak Ridge National Laboratory, Oak Ridge, TN, June 1978.

50 G. C. Smith, P. P. Holz and W. J. Stelzman, Crack Extension and Arrest Tests of Axially Flawed Steel Model Pressure Vessels, NUREG/CR-0126, ORNL/NUREG/TM-196, Oak Ridge National Laboratory, Oak Ridge, TN, October 1978.

51 R. H. Bryan, P. P. Holz, J. G. Merkle, G. C. Smith, J. E. Smith and W. J. Stelzman, Test of 6-In.-Thick Pressure Vessels. Series 3: Intermediate Test Vessel V-7B, NUREG/CR-0309, ORNL/NUREG-38, Oak Ridge National Laboratory, Oak Ridge, TN, October 1978.

Report No.

52 R. D. Cheverton, S. K. Iskander and S. E. Bolt, Applicability of LEFM to the Analysis of PWR Vessels Under LOCA-ECC Thermal Shock Conditions, NUREG/CR-0107, ORNL/NUREG-40, Oak Ridge National Laboratory, Oak Ridge, TN, October 1978.

54 R. D. Cheverton, Application of Static and Dynamic Crack Arrest Theory to TSE-4, NUREG/CR-0767, ORNL/NUREG-57, Oak Ridge National Laboratory, Oak Ridge, TN, June 1979.

DEFINITIONS

a	Crack length
a_o	Initial crack length
a_f	Final crack length
Δa	Crack extension
A	Area (energy) under a load-deflection record
b	Remaining uncracked ligament
B	Specimen thickness
C	Compliance
E	Modulus of elasticity
J	J-integral value
J_{Ic}	Critical J-integral value in the opening mode of fracture; ductile fracture toughness
T	Tearing modulus
W	Specimen width
σ_o	Uniaxial flow stress = $\frac{\sigma_{ys} + \sigma_{ts}}{2}$
σ_{ys}	Yield stress
σ_{ts}	Tensile stress

CONVERSIONS

1 in. = 25.4 mm

1 lb = 4.448 N

1 lb/in.^{2} = 6.894 x 10^3 Pa

1 $\frac{\text{in.} \cdot \text{lb}}{\text{in.}^2}$ = 0.175 kJ/m^2

THE EFFECT OF CRACK LENGTH AND SIDE GROOVES ON THE DUCTILE FRACTURE TOUGHNESS PROPERTIES OF ASTM A533 STEEL

I. SUMMARY AND CONCLUSIONS

The objective of this investigation was to determine the effect of relative crack length (a/W) and depth of side grooving on the parameters obtained from a J-R curve; these parameters are J_{Ic}, dJ/da (slope), and T (tearing modulus). The J-R curves were developed using the single specimen unloading compliance technique. In so doing, assessment of the experimental procedures for conducting an unloading compliance J-R curve test was made. The following conclusions were drawn as a result of this investigation:

1) As both a/W and the depth of side grooving increase, the degree of triaxiality through the thickness of the specimen at the crack tip increases. The resulting higher constraint tends to give straighter crack fronts with tunnelling reduced or eliminated.

2) The slope of the crack extension line on the R-curve decreased as the depth of side grooving increased.

3) The physical location of each of the two extensometers on the test specimen was different and, thus, the compliance behavior of each extensometer separately was modeled by employing different compliance relationships. The Saxena-Hudak relationship was found to work quite satisfactorily for the clip gage location at the load-line on the crack plane. A tenth order polynomial was developed to model the LVDT behavior for its location mounted on the front face straddling the load-line.

4) The compliance equations gave accurate predictions of the initial crack lengths where the crack fronts were relatively straight.

Final crack lengths were consistently underestimated because crack front tunnelling produced a deviation between the measured average crack length and that predicted by the compliance relationships. Therefore, the crack extension was consistently underestimated, but the magnitude of this difference decreased at higher a/W and % SG.

5) The R-curves developed from crack extension computed from the LVDT and clip gage compliances are different from one another for the same test. In some specimens, particularly those with smaller a/W and no side grooving, the difference was relatively large. For deeper cracks and side grooves, the differences were essentially negligible. The disparity between the R-curves developed from the clip gage and LVDT compliance is the subject of an ongoing investigation.

6) From the LVDT results, it is observed that J_{Ic} generally decreases as a/W and depth of side grooving increase.

II. INTRODUCTION

A. BACKGROUND

In recent years a considerable effort has been expended on the development of a ductile fracture toughness criterion to characterize the fracture behavior of structural materials employed at temperatures where they exhibit elastic-plastic behavior. This effort has focused, to a large extent, on the J-integral, first proposed by Rice[1,2] and later advanced as a failure criterion by Begley and Landes.[3,4] Subsequently, methodology for J-integral testing and analyses has evolved.[5-9] However, the optimum procedures and analyses have yet to be conclusively defined and standardized.

The current recommended J-integral test procedure entails determining the critical plane strain J value, J_{Ic}, from the J-R curve, which is a plot of J as a function of crack extension, Δa. The most widely used method of obtaining a J-R curve is the multiple specimen, heat tint method where a number of identical specimens (usually five to ten) are loaded to various points on the load-deflection record corresponding to different amounts of crack extension. The specimen is unloaded, heat tinted in a furnace, and broken. The tinted crack extension can then be measured. This procedure, while generally considered reliable, has the disadvantage of requiring a number of specimens which greatly increases specimen costs, analysis time and, in the case of nuclear reactors, the amount of capsule space needed to irradiate numerous specimens. Hence, there is a need for a J-integral test requiring only a single specimen. A number of techniques for detecting the onset of crack extension were reported in the literature.[10-13] A promising procedure is the monitoring of instantaneous crack length (and, consequently, crack extension) by use of unloading compliance. In this procedure, the load-deflection test is interrupted at frequent intervals, unloaded a small amount (about 10-15% of the expected maximum load), and the compliance during the unloading accurately measured. The elastic compliance can be related to the crack length by experimentally established

relationships. Consequently, a change in compliance can be related to a change in crack length. Thus, during the course of a single test, J and Δa can be monitored and used to produce an R-curve. Again, the optimum procedures and analysis for this technique need to be defined.

Another facet of J-integral testing that needs to be resolved is the effect of specimen size and geometry on the critical J value. To be a useful quantity, J_{Ic} should be a material parameter. Thus, conditions must be established in which J_{Ic} does not depend on size and geometry but represents plane strain conditions. Current recommended practice[9] suggests these conditions are met when

$$B,\ b,\ a \geq 25\ \frac{J}{\sigma_o}$$

where: B = thickness

b = remaining uncracked ligament

a = crack length

σ_o = flow stress = $\frac{\sigma_{ts} + \sigma_{ys}}{2}$

σ_{ts} = tensile stress

σ_{ys} = yield stress (0.2% offset)

The adequacy of this size criterion requires additional confirmation.

B. SCOPE

The primary objective of this investigation was to determine the effects of relative crack length, a/W, and side grooving of the remaining ligament section on the J-R curve. Side grooving is of interest because it increases the degree of stress state triaxiality ahead of the crack tip, thus imposing a larger degree of plane strain behavior. Because of the desirability of a single specimen test for nuclear reactor applications, the unloading compliance technique was employed to generate the J-R curve. As a secondary objective, the development and applicability of a second extensometer system was studied. The reason for investigating the second extensometer is the need for a redundant measurement in the event that the primary extensometer fails during a test; also, a second system might prove more suitable for unloading compliance tests conducted in a hot cell.

III. EXPERIMENTAL PROCEDURE

A. MATERIAL

The material used in this investigation was ASTM A533, Grade B (A533-B1), Class 1 steel. The material was supplied by Oak Ridge National Laboratory under the auspices of the Heavy Section Steel Technology (HSST) Program. The A533-B1 material was removed from the HSST plate 02. The heat treatment for plate 02 consisted of normalizing at 913°C (1675°F), austenitizing at 871°C (1600°F), water quenching, temperating at 663°C (1225°F), and stress relieving at 607°C (1125°F). The chemical composition, given in Table 1, and the heat treatment were reported by Childress.[14]

TABLE 1

CHEMICAL COMPOSITION OF ASTM A533-B1 STEEL (HSST PLATE 02)
(wt%)

C	Mn	Ni	Mo	Si	S	P	Cu	Fe
0.22	1.48	0.68	0.52	0.25	0.018	0.012	0.012	Balance

The specimens were removed from between the 1/4 and 3/4 thickness of the 30.48 cm (12 in.) plate. Mechanical properties[15-17] are given in Table 2. All specimens tested for this investigation were 2.54 cm (1T) compact specimens machined in the T-L orientation.

TABLE 2

STRENGTH AND IMPACT MECHANICAL PROPERTIES OF
ASTM A533-B1 STEEL AT 149°C (300°F)

Yield Strength	=	434 MPa	(63,000 psi)
Ultimate Strength	=	579 MPa	(84,000 psi)
C_V Energy	=	126 joules	(93 ft-lb)
Modulus of Elasticity, E	=	2.1×10^2 GPa	(30.7×10^6 psi)

B. TESTING AND ANALYSIS

As discussed previously, standard J-integral test procedures have not yet been established. Therefore, for this investigation, a set of guidelines for testing and analysis was agreed upon by a group of HSST contractors at a meeting in Annapolis, MD in September 1978. These guidelines were the basis for this investigation and are reviewed in this section. This will be referred to as the "baseline" analysis.

To systematically assess the effect of a/W and side grooving on the J-R curve, a test matrix was established varying a/W and the depth of side grooving. All specimens were 1T compact specimens with varying notch depths so that after fatigue precracking, three specimens each had a/W values of 0.5, 0.6, 0.7 and 0.8. In each of these groups one specimen was left with smooth surfaces (0% side grooving), one was given 45° V-shaped side grooves to a total depth of 10% (5% on each side) of the thickness, and the third was given side grooves to a total depth of 20% of the thickness. The sketch in Figure 1 shows a side grooved specimen (the smooth specimens were identical except the side groove was not present). To insure consistently sharp crack tips, all specimens were precracked in fatigue at least 2.5 mm (0.100 in.) at loads low enough that plastic flow at the crack tips was minimized.

The fracture toughness tests were conducted at 149°C (300°F) where upper shelf behavior was observed. The temperature was controlled to approximately ± 2°C in an air-circulating electrically-heated furnace. The specimen temperature was sensed with a thermocouple attached to the specimen surface. The 1T specimens were brought to test temperature in the furnace and then allowed to soak at test temperature for at least an hour prior to testing.

A J-integral test requires an accurate load versus load-point deflection record. The tests were performed on an 89.0 kN (20,000 lb) capacity closed-loop servo-controlled, hydraulic test system. The tests were conducted in stroke control at a rate of 0.5 mm (0.02 in.) per minute.. Loading clevises

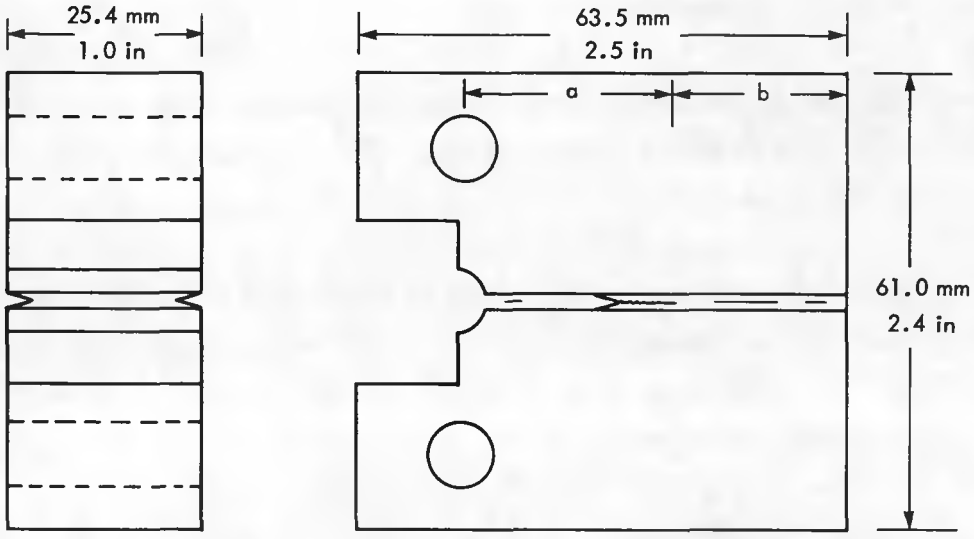

inches

a/W	B	a	b
.50	1.00	1.00	1.00
.60	1.00	1.20	.80
.70	1.00	1.40	.60
.80	1.00	1.60	.40

mm

a/W	B	a	b
.50	25.4	25.4	25.4
.60	25.4	30.5	20.3
.70	25.4	35.6	15.2
.80	25.4	40.6	10.2

HEDL 7906-063.25

FIGURE 1. Side Grooved 1T CT Specimen.

with flat bottom holes were used to test the compact specimens. The load was monitored by the system load cell. Two independent extensometer systems were used to measure displacement and provide redundancy in the event that one system failed during the test. Because of its widespread use and acceptance for J-integral testing, an electrical resistance clip gage (CG) served as the primary extensometer and was mounted on razor blade edges affixed to the crack notch at the load-line. The secondary extensometer was a linear variable differential transformer (LVDT) system, described elsewhere,[18] mounted on the front face and straddling the load-points on each side of the specimen. The signals from the LVDT's were added to give average load-line displacement measurements. The extensometer systems are shown in Figure 2.

To compute J for the compact specimens the formula developed by Rice, et al.,[6] modified for the tensile component of load after Merkle and Corten,[19] and shortened by the ASTM Task Group E24.01.09,[9] was used. This equation is

$$J = \frac{2A}{Bb}\frac{(1+\alpha)}{(1+\alpha^2)} \qquad (1)$$

where:

$$\alpha = \left[\left(\frac{2a_o}{b}\right)^2 + \frac{4a_o}{b} + 2\right]^{1/2} - \left(\frac{2a_o}{b} + 1\right) \qquad (2)$$

A = area (energy) under the load deflection record

B = thickness (net section thickness for side grooved specimens)

b = remaining uncracked ligament

a_o = initial crack length

To compute crack length from the measured compliance, the compliance equation developed by Saxena and Hudak[20] for the load-line on the crack plane was used,

$$a/W = 1.000196 - 4.06319\,U + 11.242\,U^2 - 106.043\,U^3 + 465.335\,U^4 - 650.677\,U^5 \qquad (3)$$

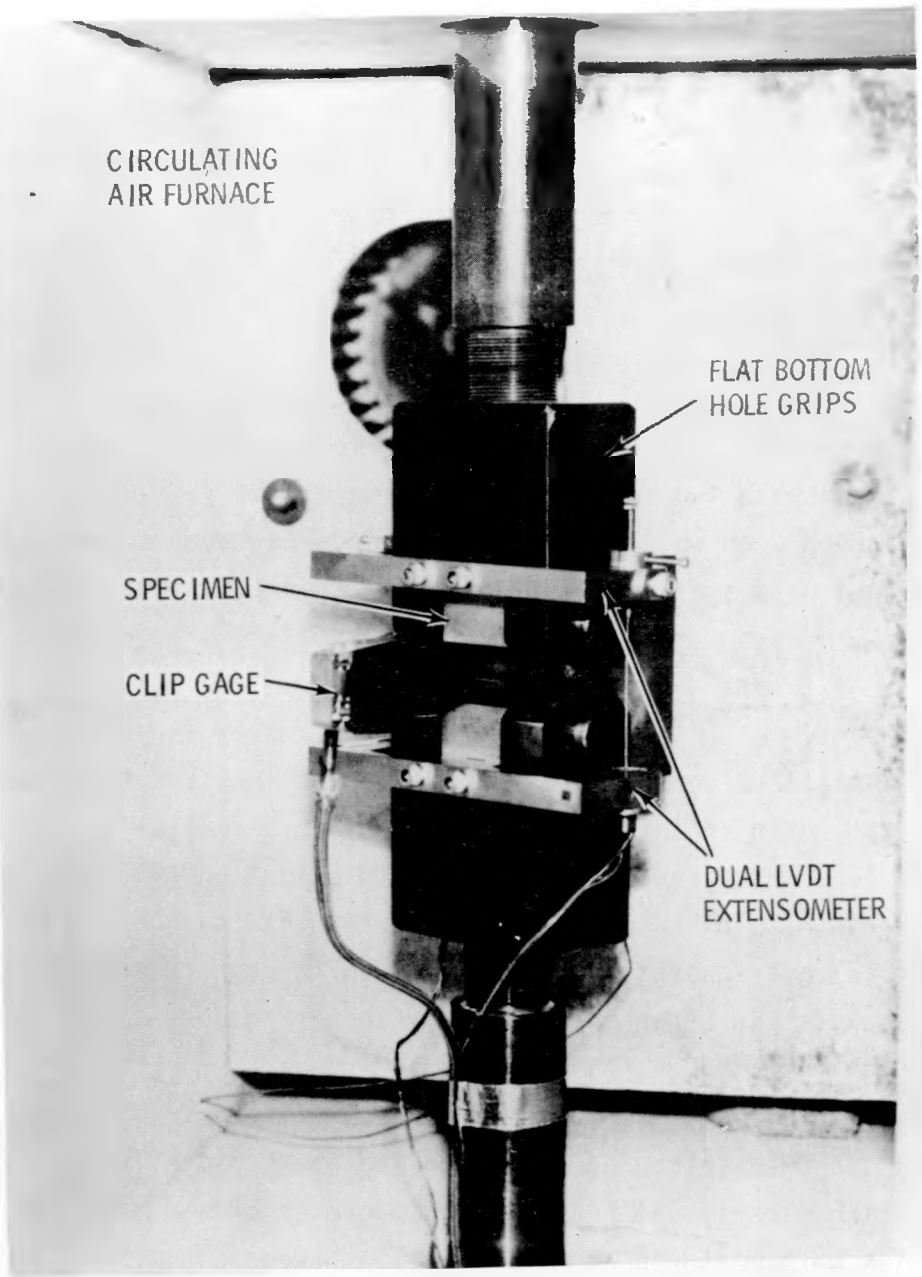

FIGURE 2. Dual LVDT and Clip Gage (CG) Extensometers Mounted on a Compact Specimen.

where: $U = \frac{1}{\sqrt{ECB} + 1}$

E = modulus of elasticity

C = compliance

For a given specimen, the initial crack length was computed from the mean of ten compliance measurements at a low load level (about 25% of expected maximum load). Crack extension was computed by subtracting this value from the crack lengths computed from compliances measured during subsequent unloadings as the test progressed.

In order to determine the J_{Ic} value, it was necessary to represent the crack tip blunting behavior and crack extension behavior. The intersection of the lines representing these two phenomena was taken as the J_{Ic} value. The baseline analysis agreed upon was based on the procedures recommended in Reference 9. The blunting line was assumed to follow the theoretical relationship

$$\Delta a = J/2\ \sigma_o \qquad (4)$$

The data points utilized for the construction of the crack extension line were those contained in an interval defined by lines parallel to the blunting line, Equation (4), but offset by 0.254 mm (0.010 in.) and 1.397 mm (0.055 in.) from the origin. The crack extension portion of the R-curve was constructed by a least squares linear regression through these points. This R-curve analysis is shown schematically in Figure 3.

After completion of a test, the specimen was heat tinted in a furnace at 649°C (1200°F) and then fractured after cooling in liquid nitrogen. The blue oxide coating clearly delineates the fatigue crack and crack extension; these quantities were measured at nine equally-spaced points along the crack front under a microscope with a vernier calibrated traveling stage at 48X magnification. The crack extension was taken as the mean of eight points: the seven interior measurements plus the average of the two surface measurements. The initial crack length as measured on the specimen fracture surface was used to compute the J values.

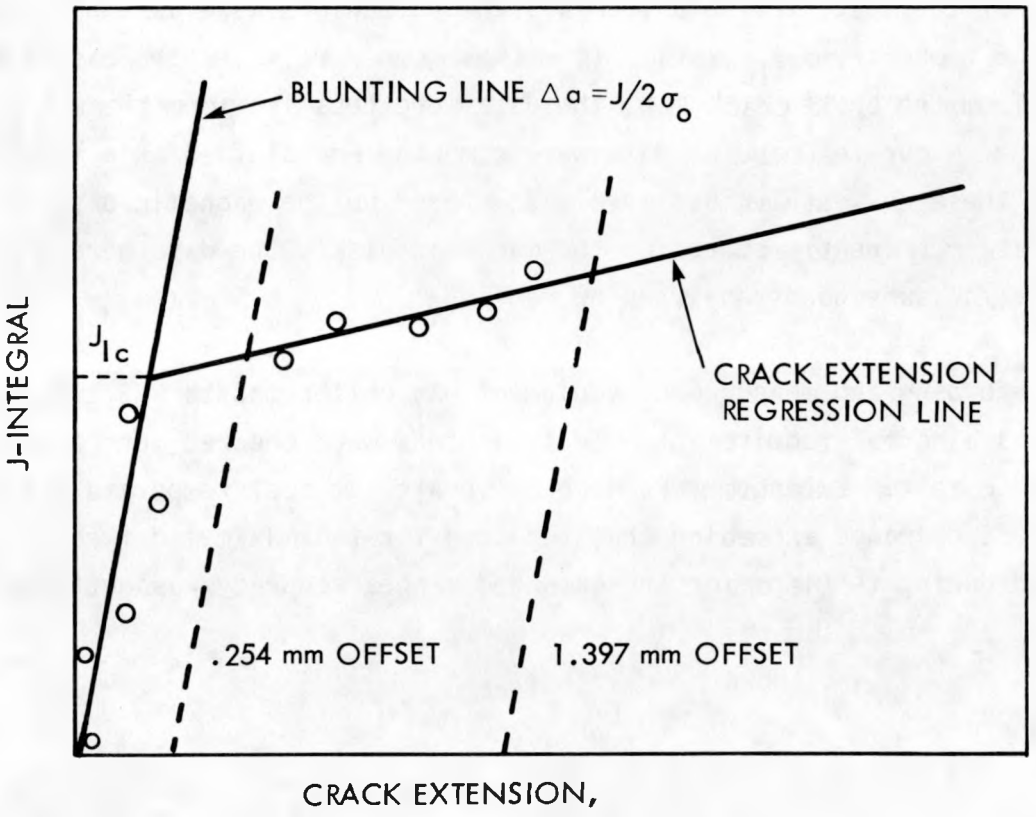

HEDL 7906-063.26

FIGURE 3. Schematic Representation of the R-Curve Analysis.

To facilitate the intricate and complicated data acquisition and computation, a mini-computer system was used. The system consisted of a magnetic tape programmable computer, X-Y plotter, thermal printer, and a magnetic disk drive for data storage. The system was programmed to accurately record load and displacements, compute the compliance, and assess the accuracy of compliance measurements. Real time computations of the compliance, the crack length, and the estimated J values were made and printed at the time of each unloading; all data were stored on a magnetic disk. Simultaneously, the X-Y recorder was autographically producing the load-deflection record. Upon completion of the test, the data from all the unloadings were assembled and plotted as a temporary J-R curve. After subsequent crack length measurements were made from the broken specimen, the data were recalled from the magnetic disk and more accurate J and Δa data were computed and plotted as a final J-R curve; these new data values were also stored on the magnetic disk. With all data permanently stored on the magnetic disks, the data were easily retrievable for subsequent analyses or replay.

All test recording and measurement equipment was calibrated to NBS traceable standards as a normal requirement. Test machines were checked for calibration prior to test. Extensometers were calibrated at test temperature and for a deflection range exceeding that required for the maximum deflection encountered during testing; for the extended ranges accuracy was better than one percent.

IV. RESULTS AND DISCUSSION

A. J-R CURVE RESULTS FROM THE BASELINE ANALYSIS

The intersection of the blunting line and crack extension line (see Figure 3) was defined as the onset of crack extension and the J value was attributed the J_{Ic} designation. Paris, et al.[21] have proposed that the slope of the crack extension line is related to a parameter which describes stable crack extension; the "tearing modulus", T, is given by

$$T = \frac{dJ}{da} \cdot \frac{E}{\sigma_o^2} \tag{5}$$

where dJ/da = slope of the crack extension line. The J_{Ic}, dJ/da, and T results for this matrix of tests are given in Table 3. Table 4 summarizes the initial crack length, final crack length, and crack extension computed from the clip gage compliance and from direct measurement. The R-curve constructions are shown in Figures 4 through 15. Figure 16 shows the fracture surfaces of all specimens in the test matrix.

A significant observation, seen in Figure 16, is that the crack front becomes straighter with crack tunnelling reduced or eliminated as a/W and depth of side grooving (% SG) increase. This indicates that the through-the-thickness constraint increased with the greater depth of side grooving and also with increased crack length. As a result of the increased constraint, the slope of the R-curve, dJ/da, and, consequently, the tearing modulus, T, tended to decrease as the depth of side grooving increased; however, a consistent trend in dJ/da or T as a/W increased was not conclusively discernible. The J_{Ic} results for these tests (Table 3) also do not show a distinct trend with either % SG or a/W but rather tend to vary over a large range. As shown in Table 4, the crack lengths computed from the elastic unloading compliance using the Saxena-Hudak relationship, Equation (3), for the initial fatigue cracks (straight crack fronts) were generally in good agreement with the direct nine-point measurement. Agreement after crack extension occurred was still good when crack fronts remained straight, but deteriorated when

TABLE 3

J-R CURVE RESULTS FROM THE CLIP GAGE EXTENSOMETER

a/W \ % Side Groove		0%	10%	20%
0.5	a/W	0.527	0.519	0.515
	J_{Ic}, kJ/m^2 (in-lb/in^2)	187.8 (1073)	242.0 (1383)	220.3 (1259)
	dJ/da, MPa (lb/in^2)	271 (39,239)	201 (29,159)	149 (21,572)
	T	215	160	118
0.6	a/W	0.615	0.619	0.623
	J_{Ic}, kJ/m^2 (in-lb/in^2)	395.2 (2258)	196.4 (1122)	253.0 (1446)
	dJ/da, MPa (lb/in^2)	175 (25,343)	228 (33,130)	142 (20,663)
	T	139	182	113
0.7	a/W	0.723	0.723	0.720
	J_{Ic}, kJ/m^2 (in-lb/in^2)	350.0 (2000)	226.3 (1293)	184.3 (1053)
	dJ/da, MPa (lb/in^2)	198 (28,658)	217 (31,511)	170 (24,639)
	T	157	173	135
0.8	a/W	0.855	0.812	0.812
	J_{Ic}, kJ/m^2 (in-lb/in^2)	207.7 (1187)	215.1 (1229)	219.8 (1256)
	dJ/da, MPa (lb/in^2)	359 (52,116)	203 (29,389)	174 (25,185)
	T	286	161	138

TABLE 4

COMPARISON OF COMPUTED AND MEASURED CRACK LENGTHS
BASED ON CLIP GAGE EXTENSOMETER RESULTS

a/W	% SG	0% Meas	0% CG	10% Meas	10% CG	20% Meas	20% CG
0.5	a_o	1.0530	1.0369	1.0387	1.0269	1.0290	1.0356
	a_f	1.1603	1.1198	1.1437	1.1308	1.1150	1.1272
	Δa	0.1073	0.0829	0.1050	0.1039	0.0860	0.0916
0.6	a_o	1.2301	1.2328	1.2384	1.2371	1.2461	1.2570
	a_f	1.3244	1.2990	1.3281	1.3101	1.3280	1.3355
	Δa	0.0943	0.0662	0.0897	0.0731	0.0819	0.0785
0.7	a_o	1.4464	1.4481	1.4468	1.4481	1.4391	1.4491
	a_f	1.5467	1.5262	1.5291	1.5123	1.5083	1.5186
	Δa	0.1003	0.0781	0.0823	0.0642	0.0692	0.0695
0.8	a_o	1.7096	1.7112	1.6249	1.6309	1.6232	1.6383
	a_f	1.7676	1.7503	1.7063	1.6961	1.7013	1.7079
	Δa	0.0580	0.0391	0.0814	0.0653	0.0781	0.0696

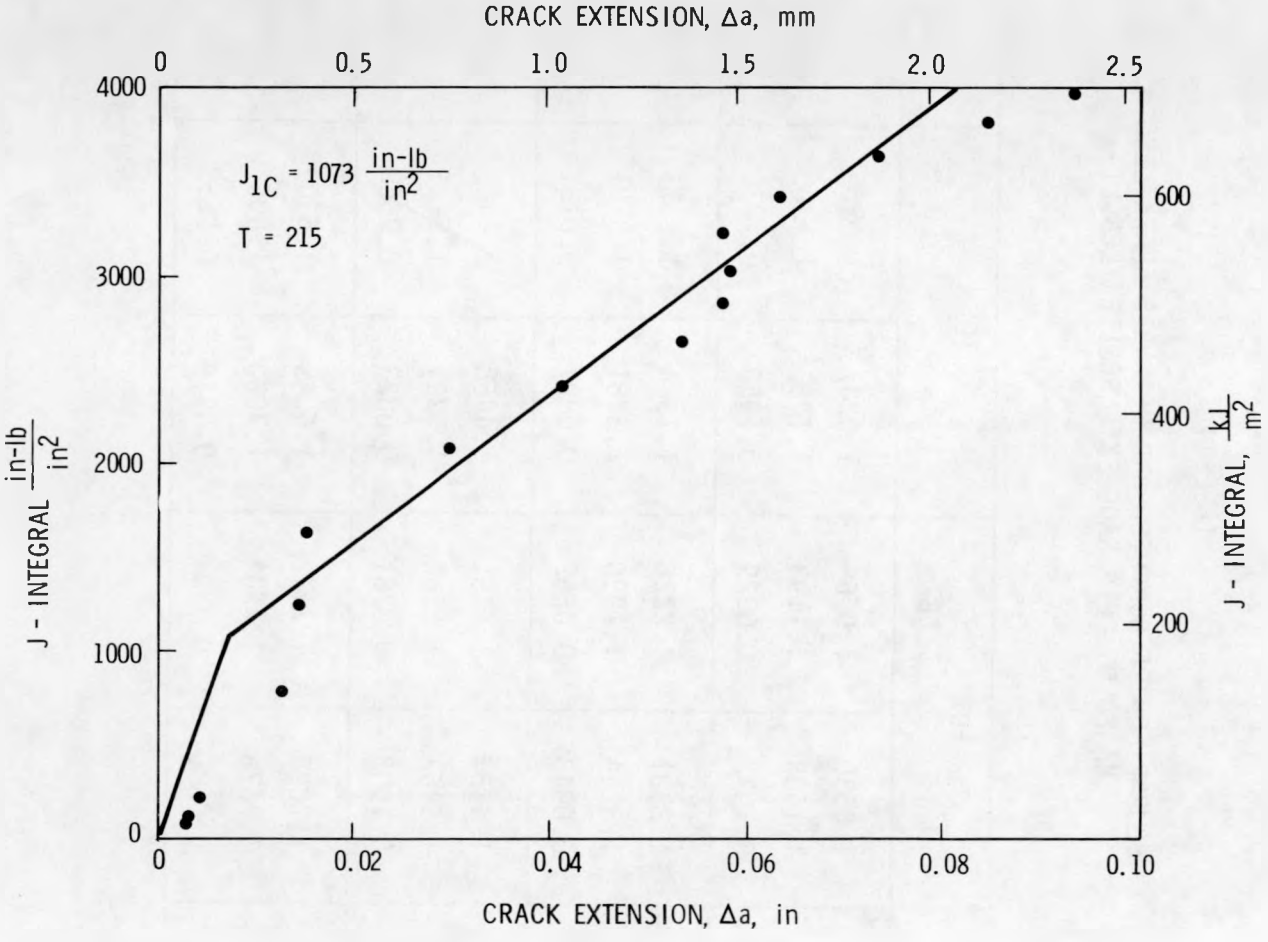

FIGURE 4. R-Curve from the Clip Gage for Matrix Specimen 02GAA1-47 (a/W = 0.5, % SG = 0).

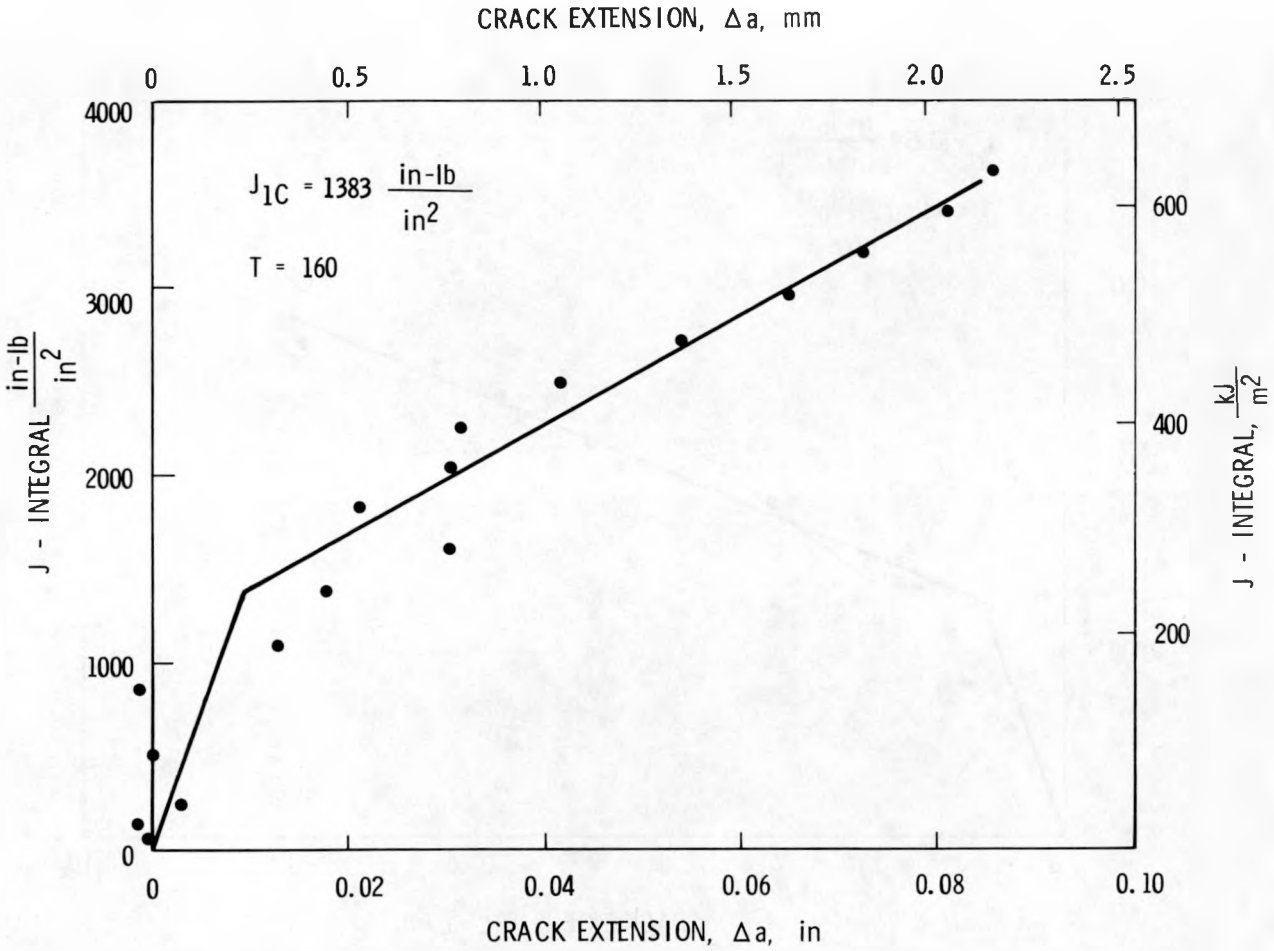

FIGURE 5. R-Curve from the Clip Gage for Matrix Specimen 02GAA1-34 (a/W = 0.5, % SG = 10).

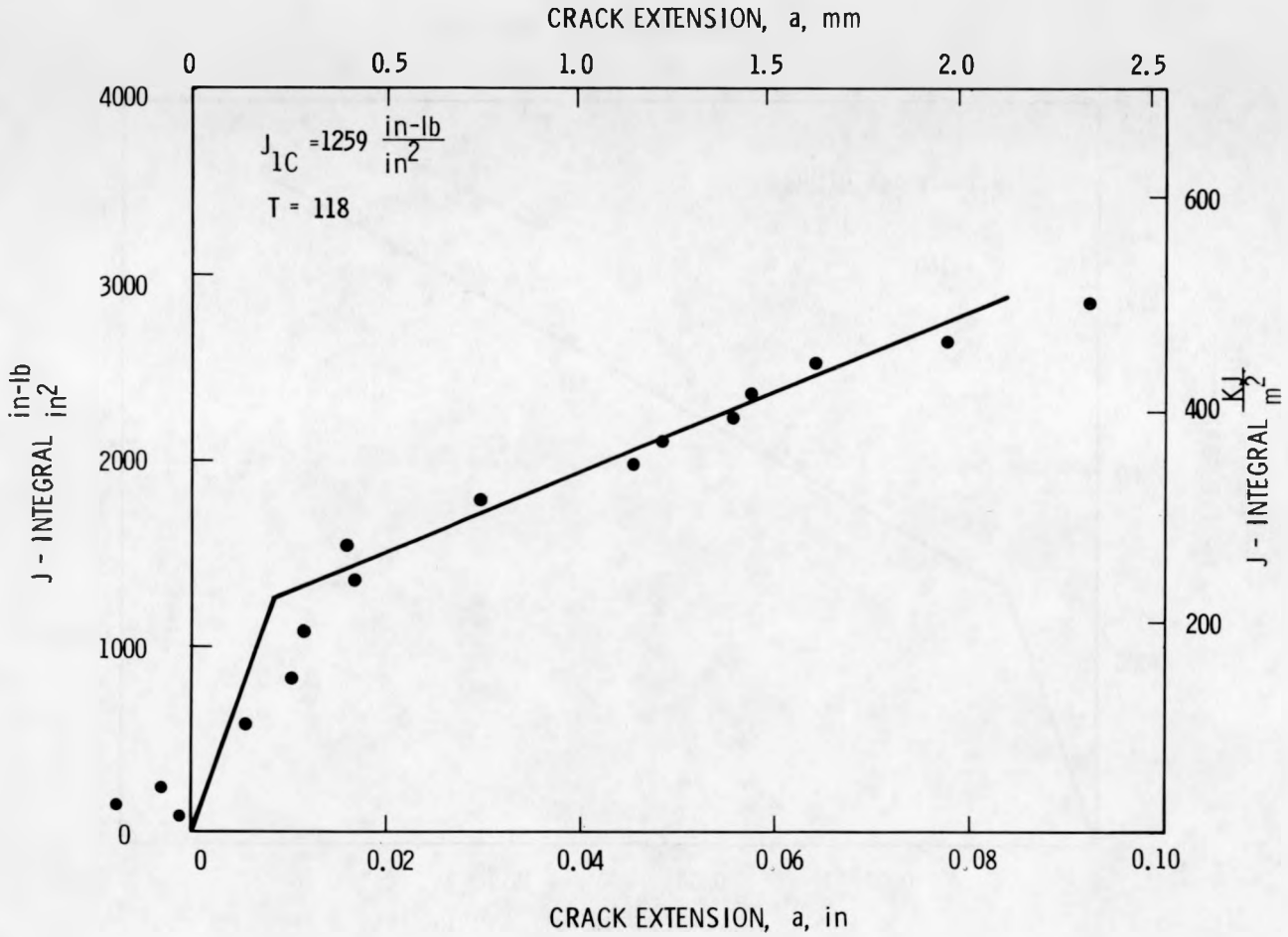

FIGURE 6. R-Curve from the Clip Gage for Matrix Specimen 02GAA1-36 (a/W = 0.5, % SG = 20).

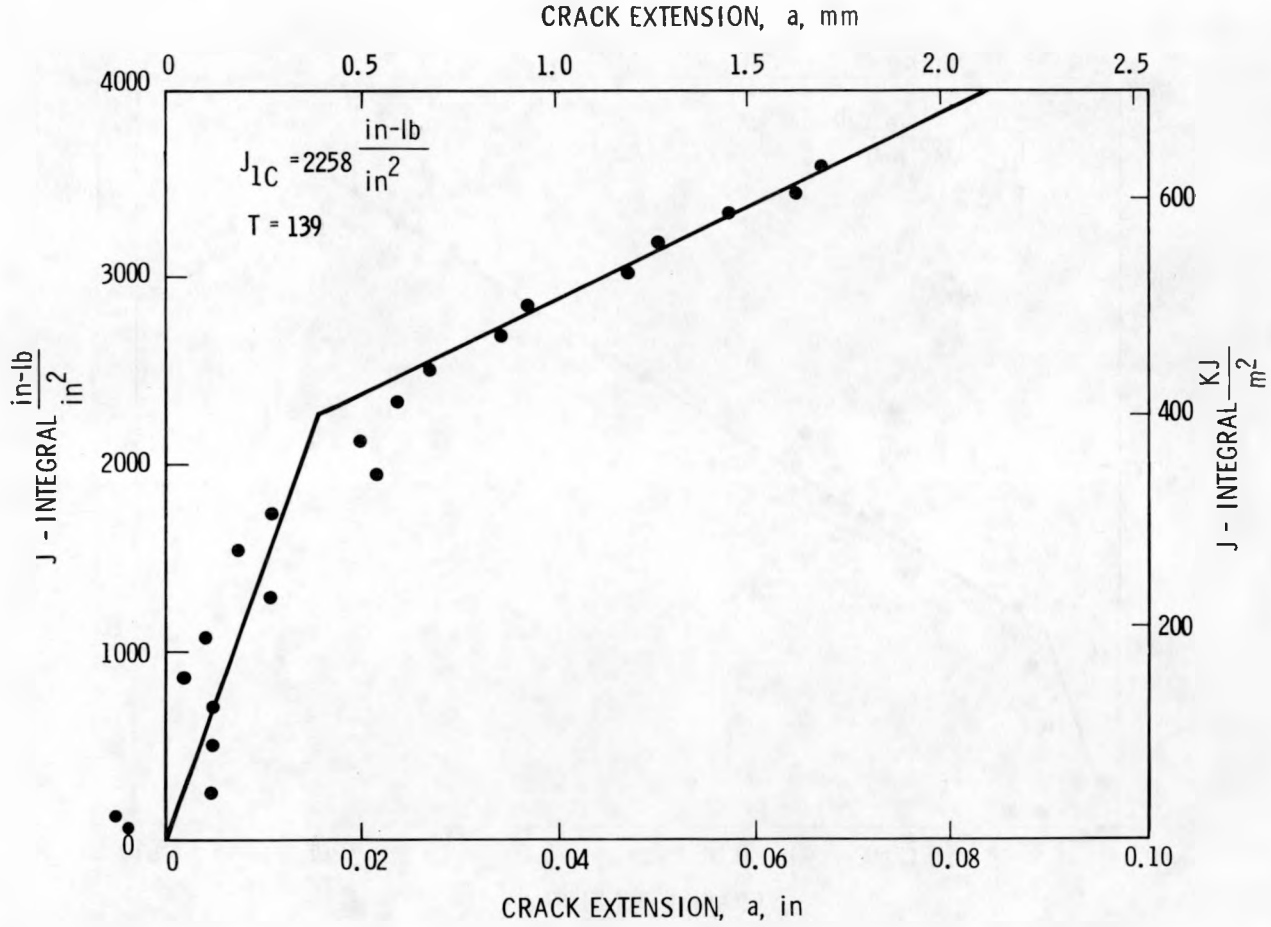

FIGURE 7. R-Curve from the Clip Gage for Matrix Specimen 02GAA1-143 (a/W = 0.6, % SG = 0).

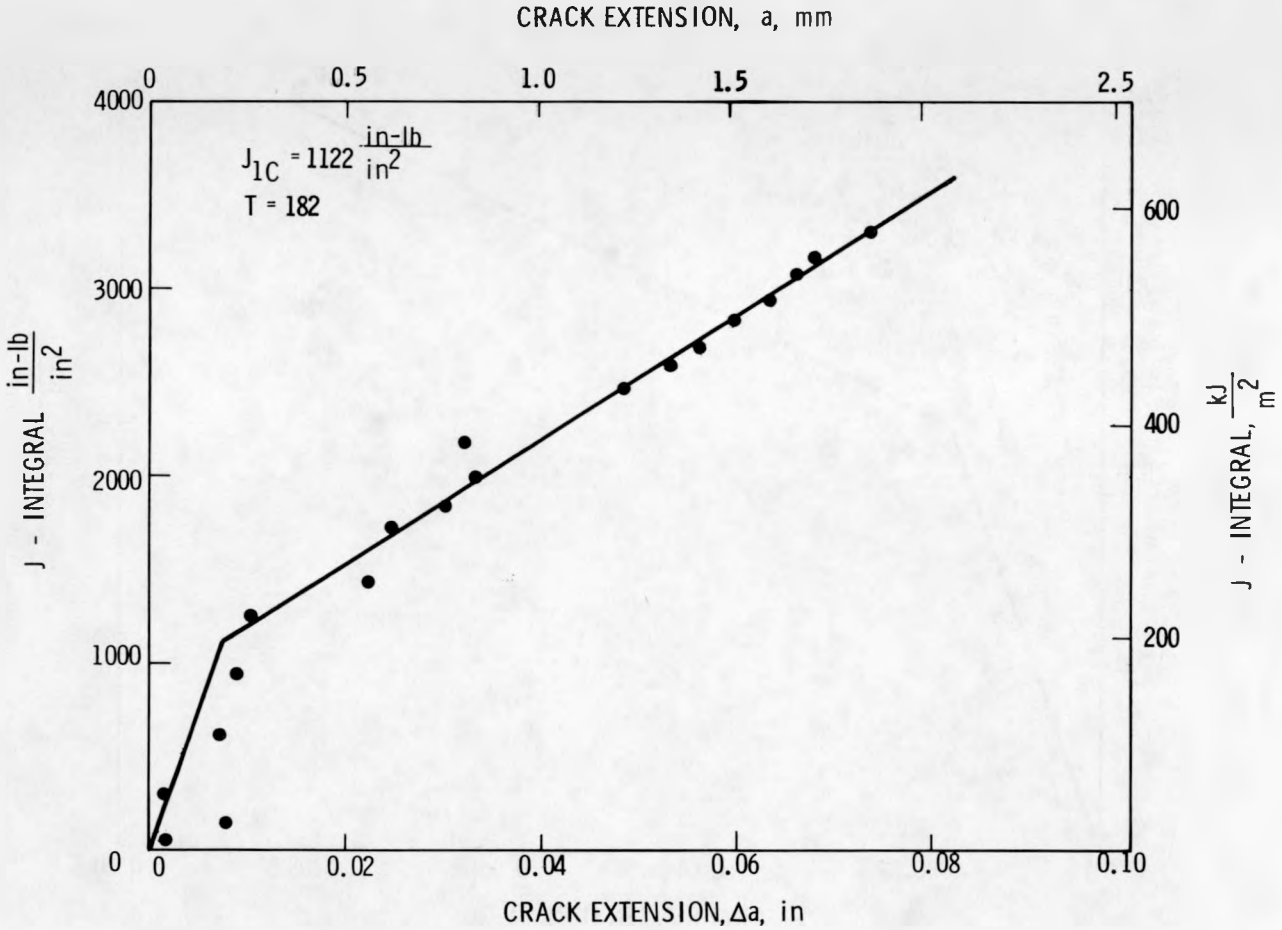

FIGURE 8. R-Curve from the Clip Gage for Matrix Specimen 02GAA1-38 (a/W = 0.6, % SG = 10).

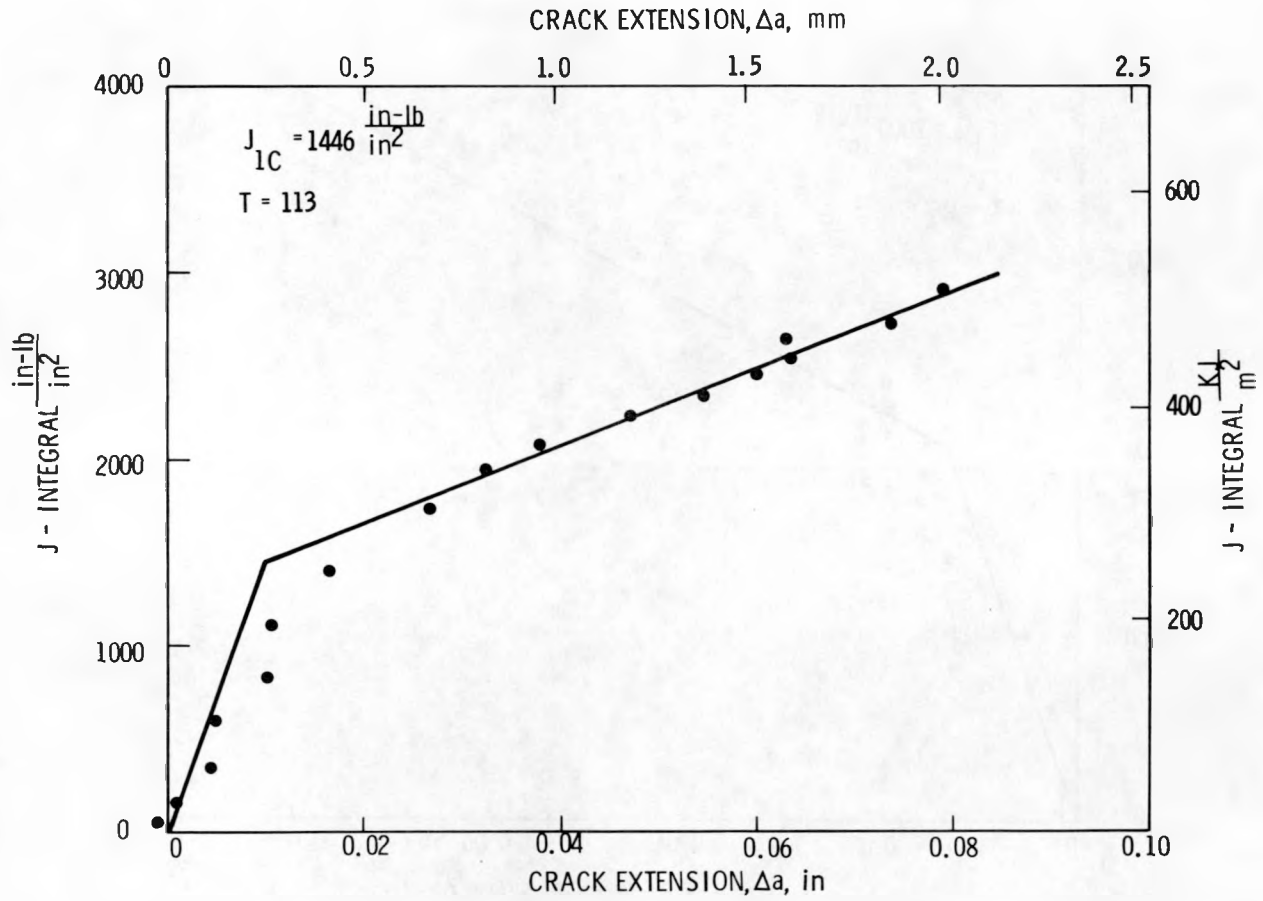

FIGURE 9. R-Curve from the Clip Gage for Matrix Specimen 02GAA1-40 (a/W = 0.6, % SG = 20).

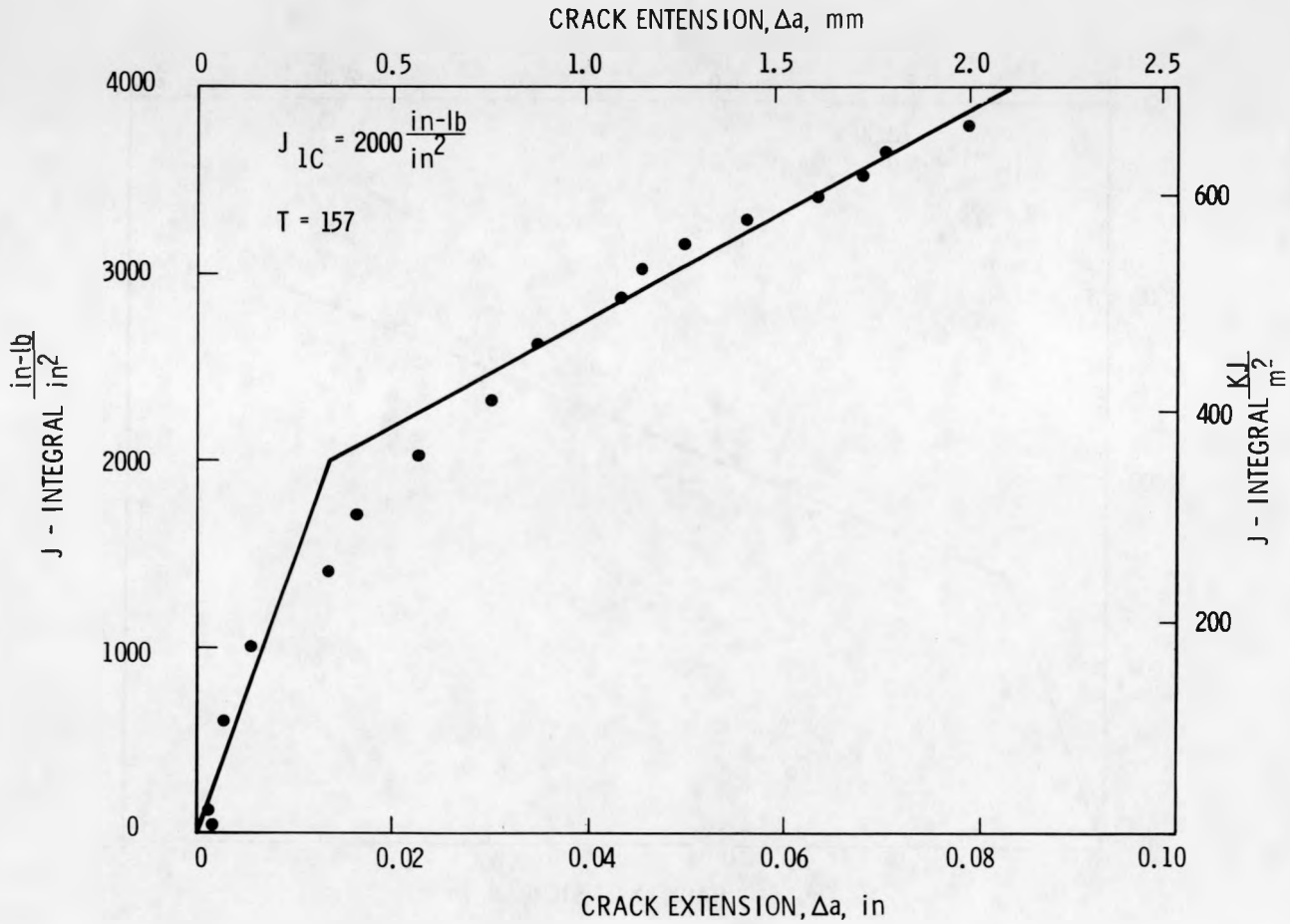

FIGURE 10. R-Curve from the Clip Gage for Matrix Specimen 02GA603 (a/W = 0.7, % SG = 0).

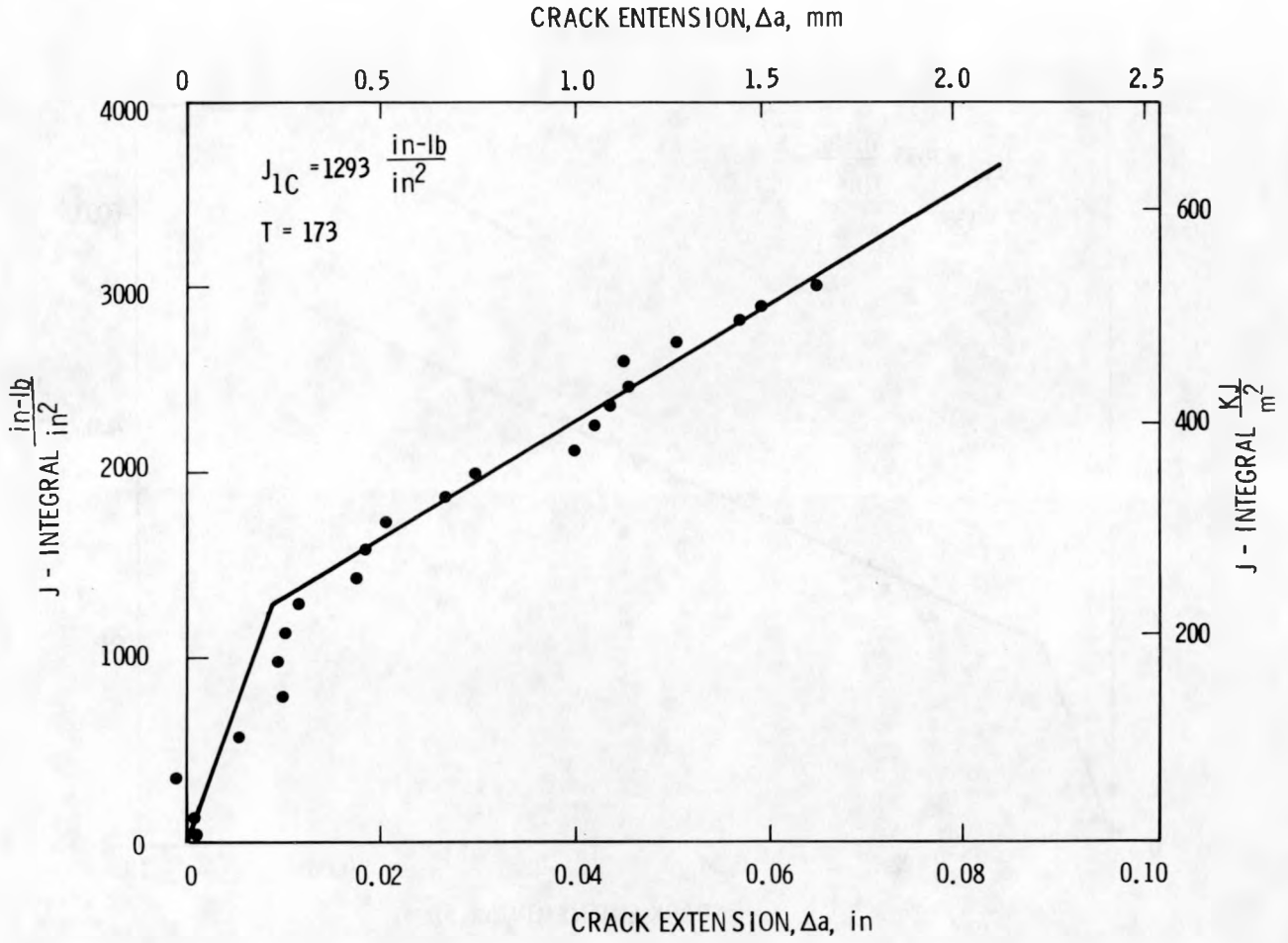

FIGURE 11. R-Curve from the Clip Gage for Matrix Specimen 02GAA1-41 (a/W = 0.7, % SG = 10).

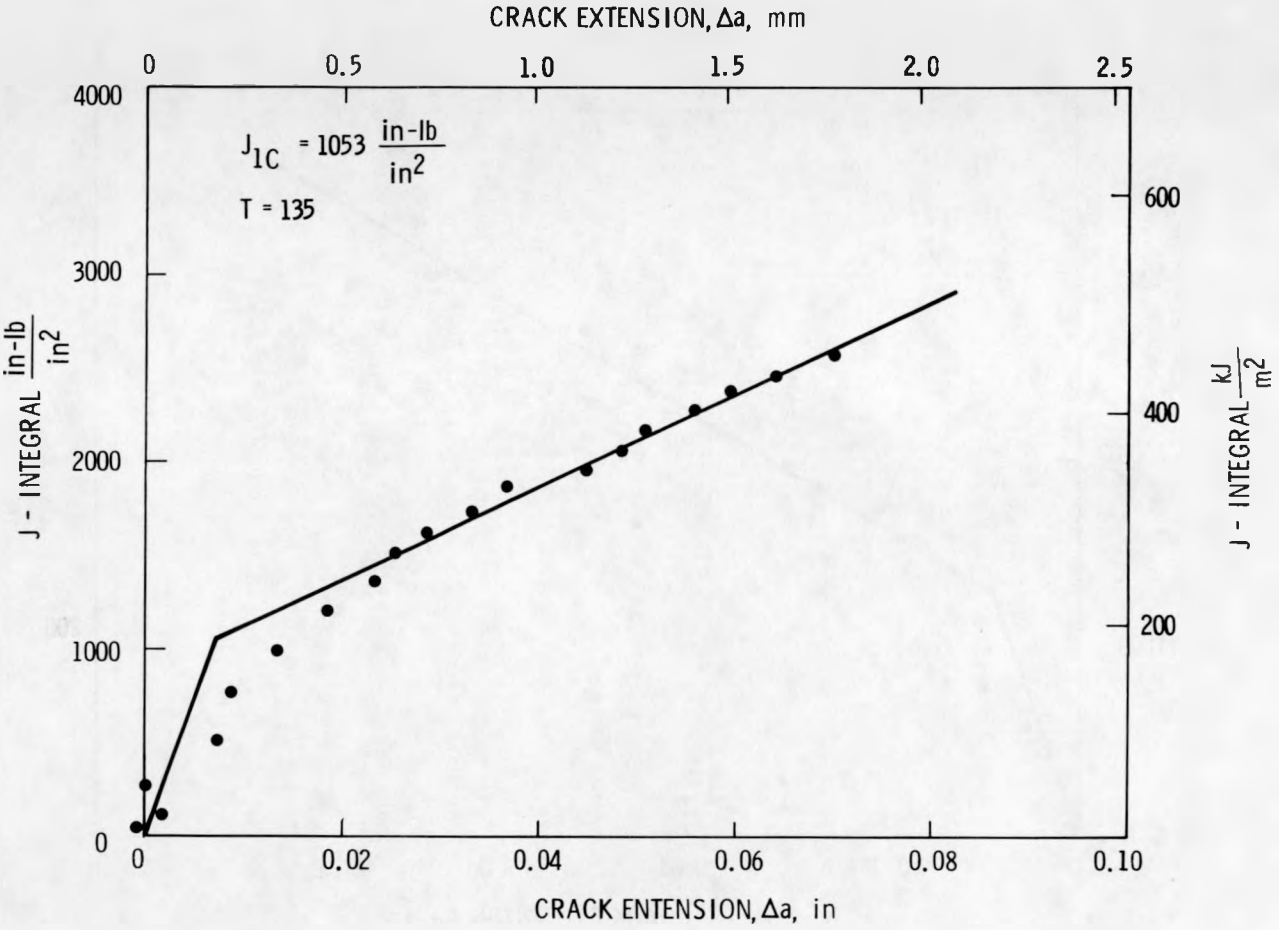

FIGURE 12. R-Curve from the Clip Gage for Matrix Specimen 02GAA1-43 (a/W = 0.7, % SG = 20).

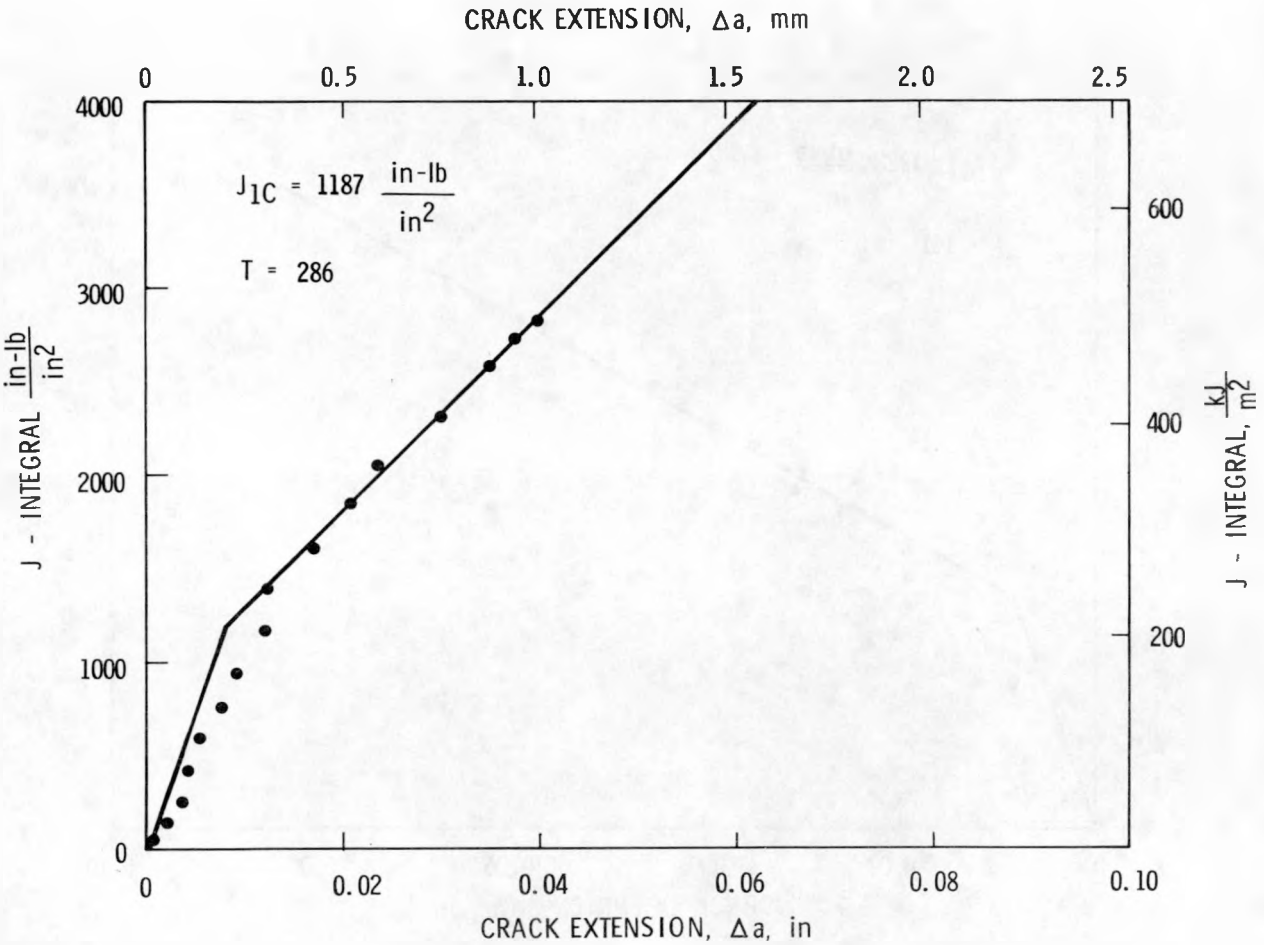

FIGURE 13. R-Curve from the Clip Gage for Matrix Specimen 02GAA1-28 (a/W = 0.8, % SG = 0).

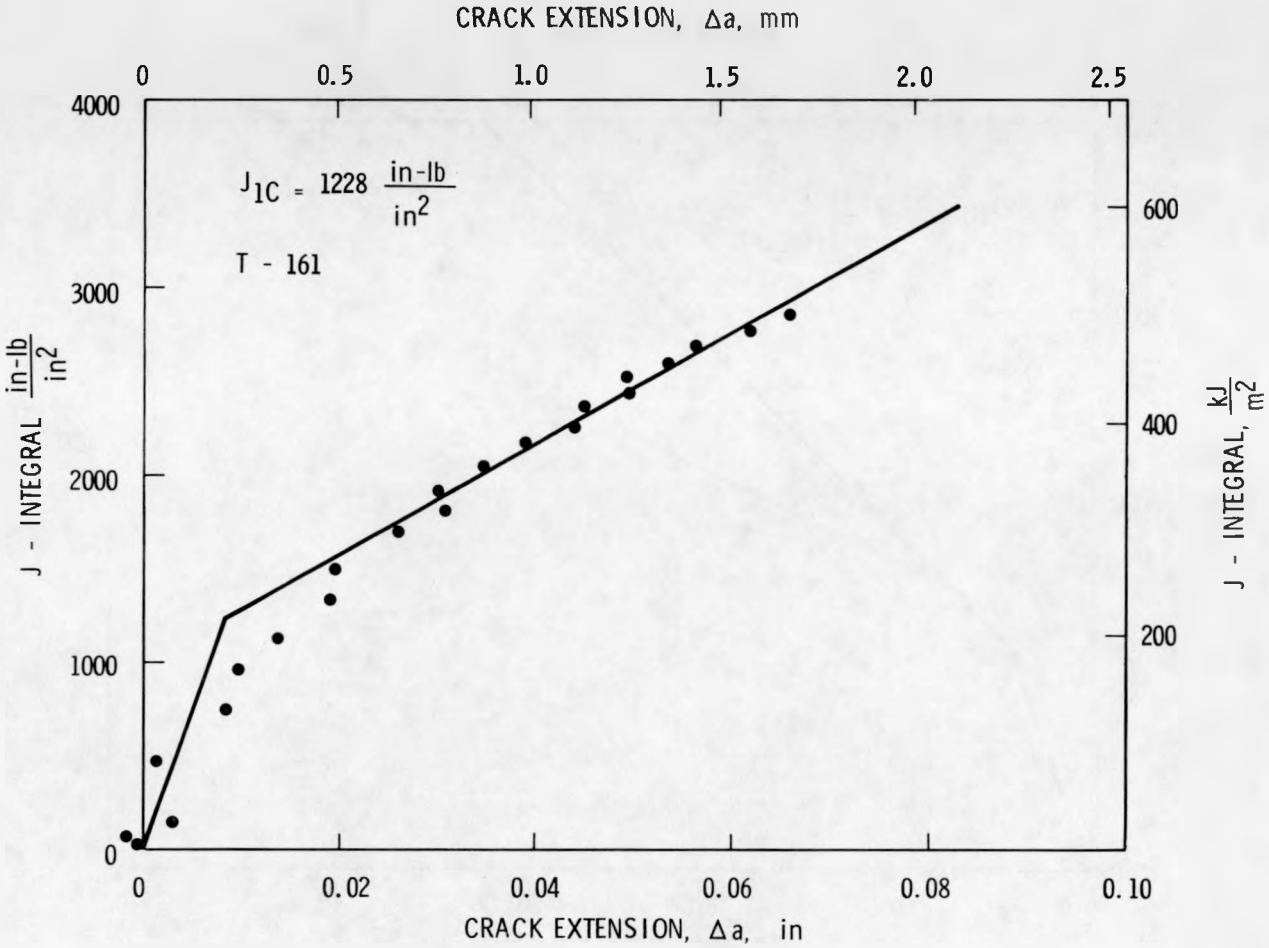

FIGURE 14. R-Curve from the Clip Gage for Matrix Specimen 02GAA1-45 (a/W = 0.8, % SG = 10).

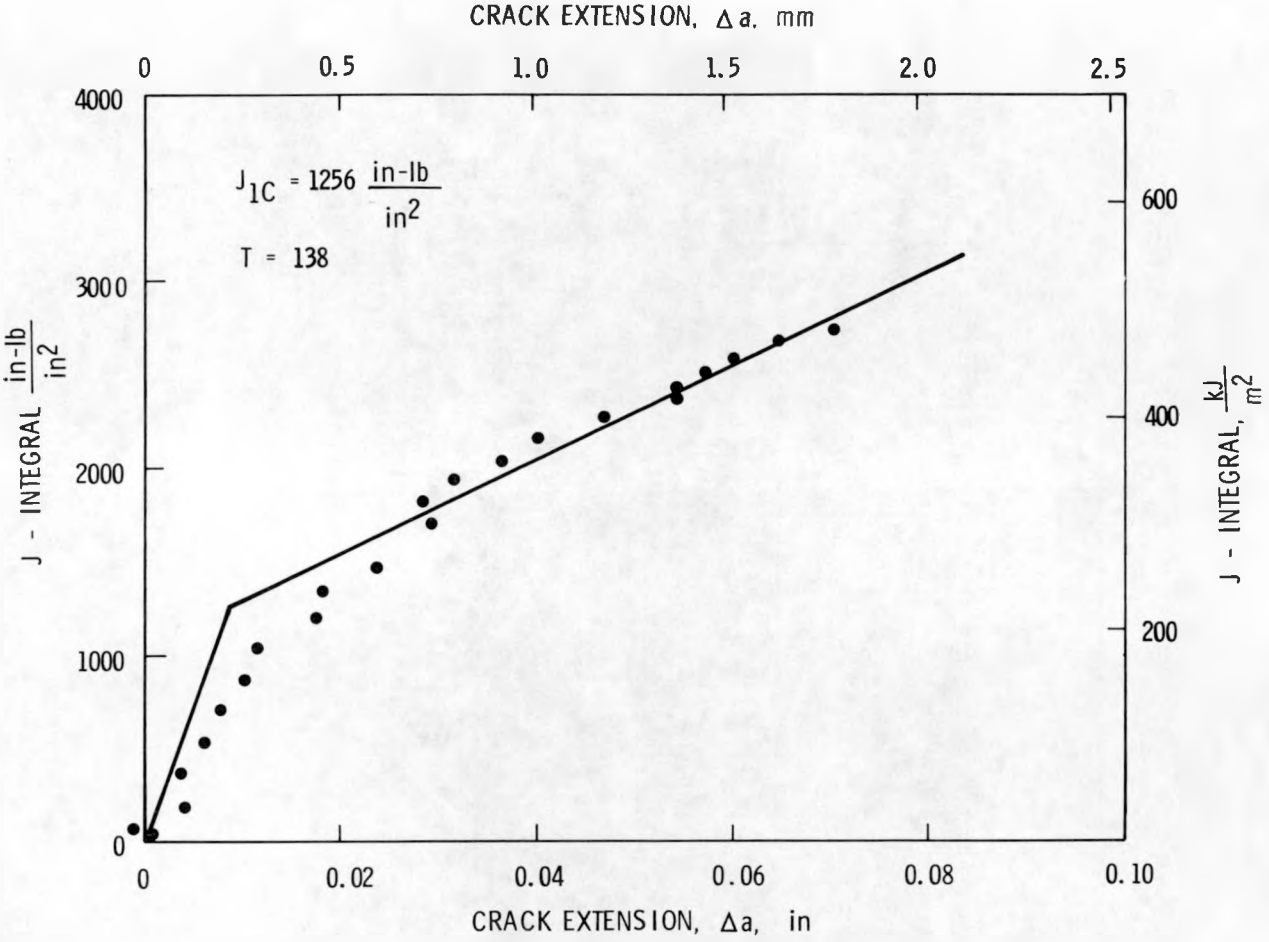

FIGURE 15. R-Curve from the Clip Gage for Matrix Specimen 02GAA1-46 (a/W = 0.8, % SG = 20).

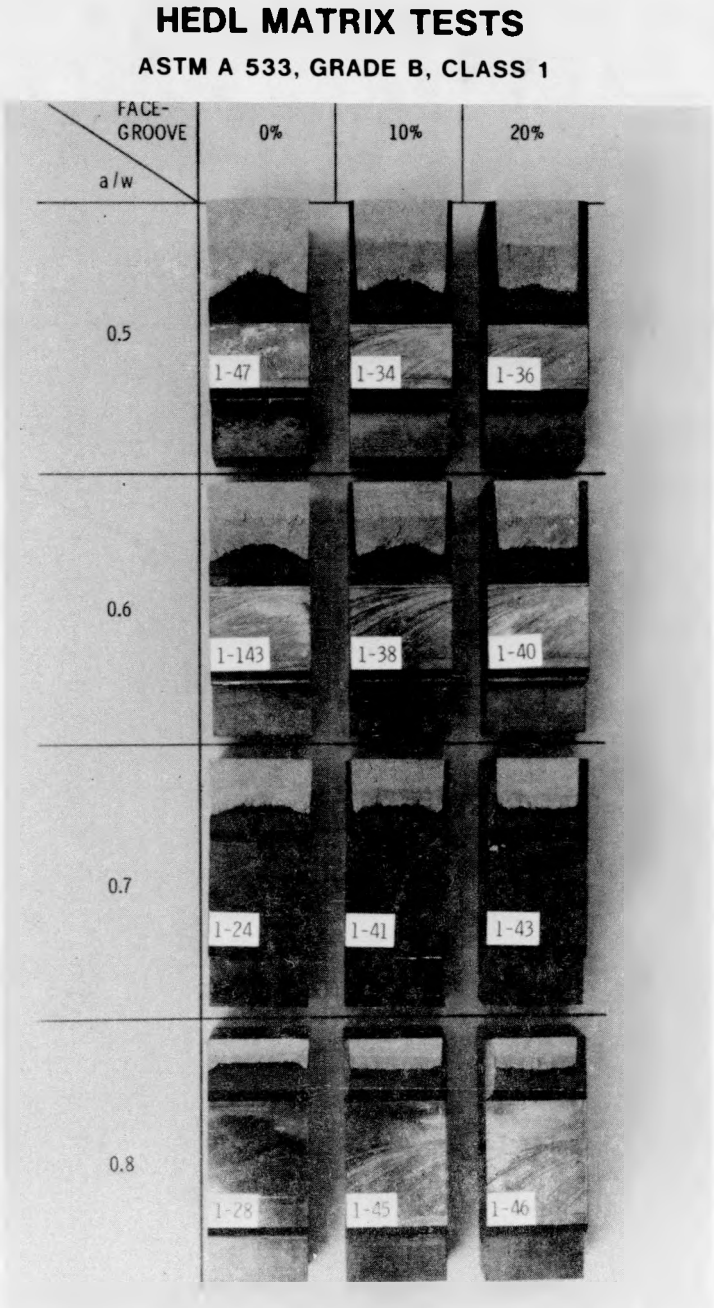

FIGURE 16. Heat Tinted Fracture Surfaces for the Test Matrix Specimens.

crack extension manifested itself by crack front tunnelling near the mid-thickness of the specimen. The trends suggest that to obtain consistent plane strain ductile fracture toughness properties, it may be necessary to employ side grooves or perhaps deeper cracks.

The absence of consistent trends in these test results is believed to be the effect of shortcomings in the accepted data analysis procedures. Specifically, the applicability of the theoretical blunting line, Equation (4), as a model for the unloading compliance-based crack length during crack-opening-stretch is questioned. This can be observed in the R-curves of Figures 4 through 15. In most of the R-curves, the experimental data points for the blunting portion of the R-curve do not lie on the theoretical blunting line, Equation (4). The reason is simply that Equation (4) yields a quantity which is a physical displacement at the crack tip due to local plastic deformation, while the compliance relationship, Equation (3), relates the elastic compliance with physical crack length. Thus, there seems to be no intrinsic reason for the apparent crack extension resulting from the crack tip blunting phenomenon to be quantitatively described by the elastic compliance measurement in the same way it is in the multiple specimen heat tint measurement. Some revisions in describing blunting as detected by the compliance method may be appropriate to effectively characterize the onset of crack extension. Alternatives for the blunting line described by Equation (4) will be studied in subsequent work.

B. J-R CURVE RESULTS USING THE LVDT EXTENSOMETER SYSTEM

The dual LVDT extensometer system described earlier was studied to assess its applicability for unloading compliance J-R curve tests. The LVDT system was intended to be a redundant extensometer in the event that the clip gage failed during the test of an irradiated specimen. However, if its applicability is demonstrated, it may eventually be used as the primary system because of its ease of use with manipulators in a hot cell compared to the clip gage.

Good agreement between computed crack lengths from the LVDT and clip gage extensometers requires the use of compliance relationships appropriate for the specific extensometer location. The Saxena-Hudak relationship, Equation (3), was used with good results for the clip gage compliance data because it was compatible with clip gage location. As expected, the Saxena-Hudak relationship did not satisfactorily model the compliance behavior of the LVDT which was located on the front face.

To account for the location of the LVDT system, a separate compliance relationship was developed for the initial crack length data points from the LVDT; the clip gage results were still modeled by the Saxena-Hudak relationship. The LVDT data were fit to a tenth order polynomial given by

$$a/W = A + BU + CU^2 + DU^3 + EU^4 + FU^5 + GU^6 + HU^7 + IU^8 + JU^9 + KU^{10} \qquad (6)$$

where:

$A = 1.99703336 \times 10^{-1}$
$B = 1.02757992 \times 10^{-2}$
$C = -9.21439591 \times 10^{-5}$
$D = 4.98545748 \times 10^{-7}$
$E = -1.67770409 \times 10^{-9}$
$F = 3.54602681 \times 10^{-12}$
$G = -4.57086111 \times 10^{-15}$
$H = 3.20604500 \times 10^{-18}$
$I = -6.86811088 \times 10^{-22}$
$J = -4.66766016 \times 10^{-25}$
$K = 2.34185204 \times 10^{-28}$

This relationship is valid in the interval $0.5 \leq a/W < 0.86$ and provides a good fit for the initial crack length data as seen in Figure 17. This relationship was developed from data obtained from 1T specimens and as yet requires verification for other sizes.

In Figure 17, the experimental data points were plotted as normalized compliance, ECB, as a function of measured a/W (recall that the weighted nine-point average measurement technique was used). To demonstrate the similarity of this relationship to the Saxena-Hudak relationship, Figure 18 shows the normalized clip gage crack length with the Saxena-Hudak relationship superimposed. In both figures, the initial and final crack lengths from the

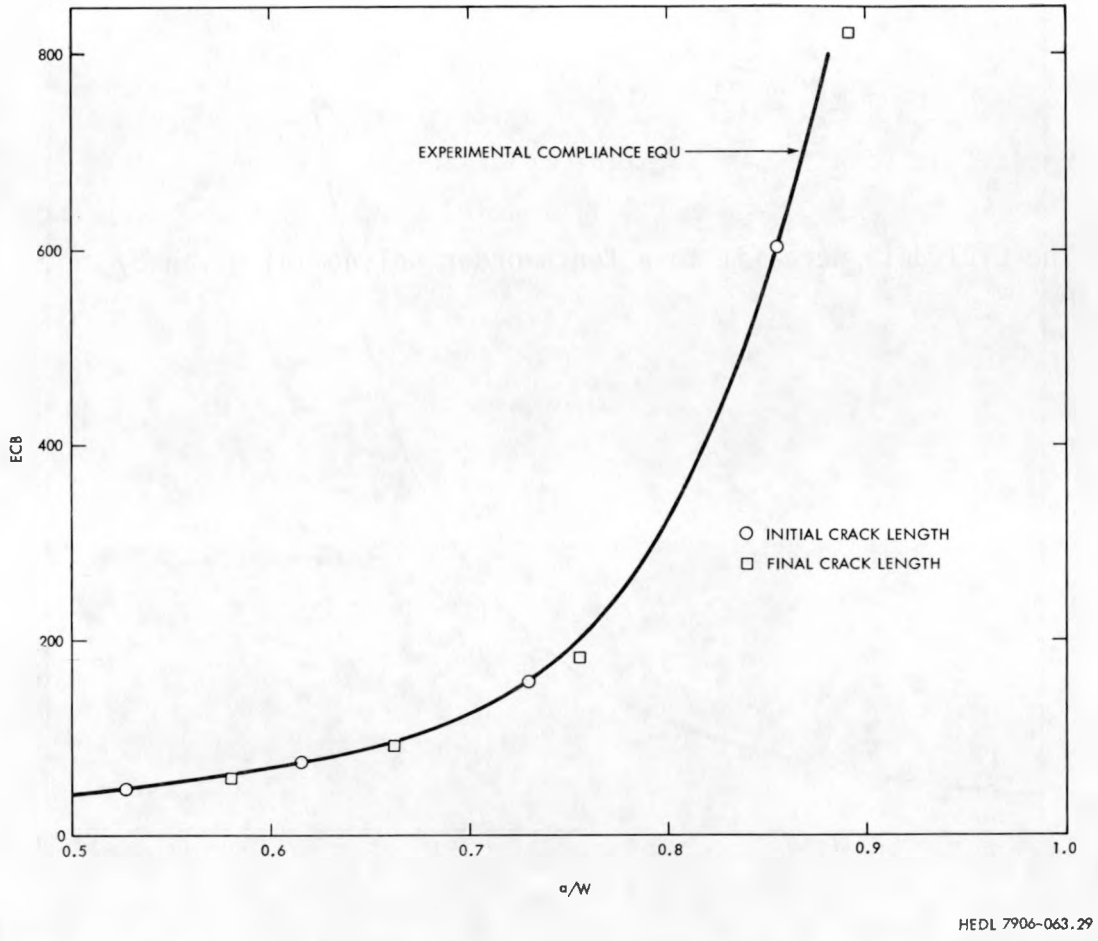

FIGURE 17. Experimental LVDT Compliance Data from the Smooth Matrix Specimens (% SG = 0) with an Empirical 10th Order Polynomial Equation Fit Through the Initial Crack Length Data.

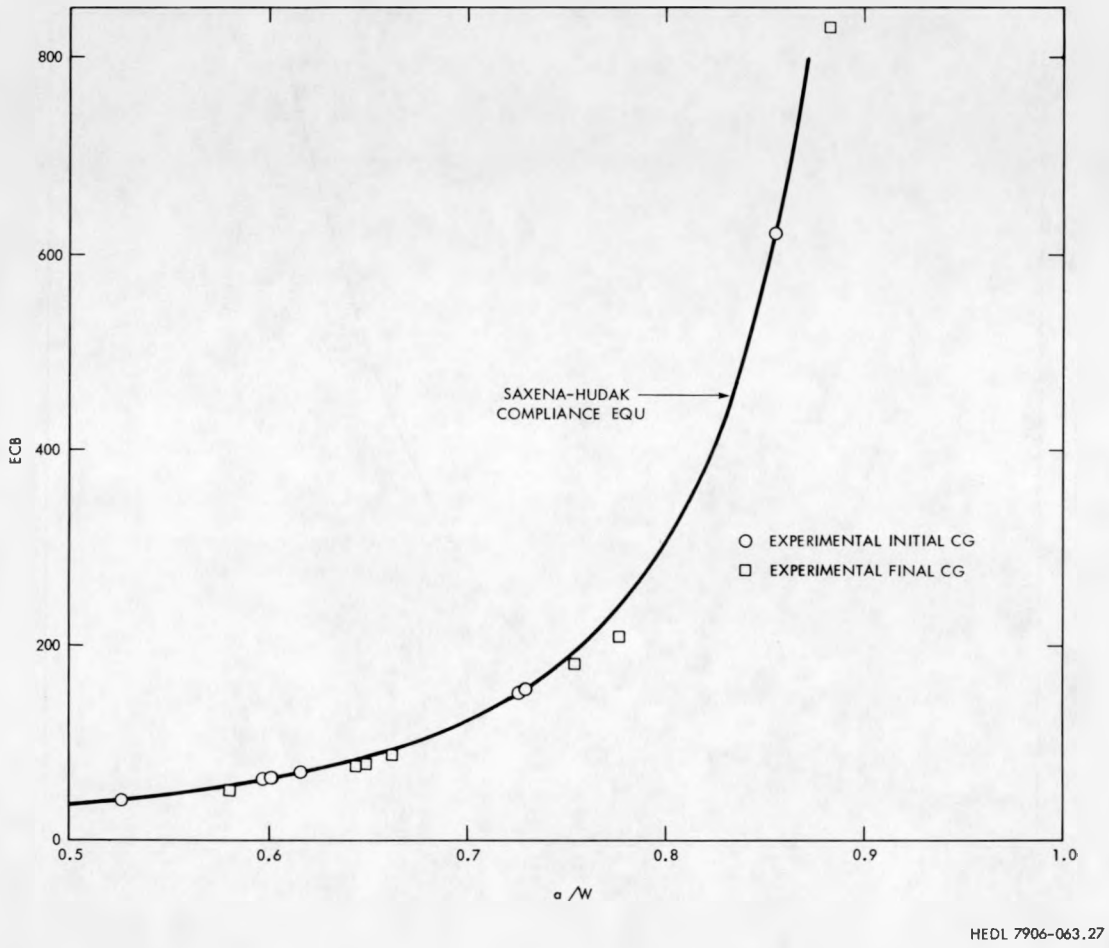

FIGURE 18. Experimental Clip Gage Compliance Data from the Smooth Matrix Specimens (% SG = 0) Compared with the Saxena-Hudak Relationship.

experimental data are plotted to observe the effect of crack tunnelling. To keep the comparison simple, only the data from smooth specimens (% SG = 0) were plotted. In both figures the initial measured crack lengths, where the crack fronts are relatively straight, show good agreement with their respective compliance equation. The final crack lengths deviate from the compliance relationships as the crack fronts bow out or tunnel. Therefore, the final crack lengths predicted from the compliance relationships are underestimated compared to the measured weight, nine-point average. Thus, it is apparent that after crack front tunnelling begins, the compliance relationships deteriorate as models for compliance response to crack extension.

All LVDT extensometer data was analyzed using Equation (6). Table 5 summarizes the J_{Ic}, dJ/da, and T results obtained from the LVDT extensometers. Initial crack length, final crack length, and crack extension for the LVDT extensometer and from the weighted nine-point average measurement are presented in Table 6. The R-curves developed from the LVDT data using the experimental compliance equation for the test matrix are shown in Figures 19 through 30.

Some trends were discernible from the data obtained from the LVDT extensometers. In general, J_{Ic} decreases as a/W and % SG increase and dJ/da and T decrease as % SG increases (see Table 5). These observations, coupled with the increasingly straighter crack fronts observed as a/W and % SG increase, support the assertion that plane strain behavior is being approached as a/W and % SG increase. Table 6 shows that, similar to the clip gage, the crack length predicted by the compliance equation is in better agreement with the weighted nine-point average measured crack extension for the initial crack length where the crack front is relatively straight. In Figures 19 through 30, most of the R-curves, like those from the clip gage, reveal that the data points from the blunting portion of the R-curve do not lie on the theoretical blunting line, Equation (4).

While additional work is needed on the extensometer systems, the results reported herein indicate that the LVDT system modeled by the experimental

TABLE 5

J-R CURVE RESULTS BASED ON EXPERIMENTAL COMPLIANCE RELATIONSHIP FOR THE LVDT

a/W \ % Side Groove		0%	10%	20%
0.5	a/W	0.527	0.519	0.515
	J_{Ic}, kJ/m^2 (in-lb/in^2)	426.6 (2436)	322.1 (1839)	272.1 (1554)
	dJ/da, MPa (lb/in^2)	188 (27,327)	217 (31,515)	143 (20,694)
	T	150	173	113
0.6	a/W	0.615	0.619	0.623
	J_{Ic}, kJ/m^2 (in-lb/in^2)	330.6 (1888)	314.0 (1793)	264.8 (1512)
	dJ/da, MPa (lb/in^2)	199 (28,819)	163 (23,637)	146 (21,150)
	T	158	130	116
0.7	a/W	0.723	0.723	0.720
	J_{Ic}, kJ/m^2 (in-lb/in^2)	342.7 (1957)	272.3 (1555)	235.9 (1347)
	dJ/da, MPa (lb/in^2)	216 (31,398)	185 (26,904)	157 (22,828)
	T	172	147	125
0.8	a/W	0.855	0.812	0.812
	J_{Ic}, kJ/m^2 (in-lb/in^2)	140.1 (800)	206.3 (1178)	215.9 (1231)
	dJ/da, MPa (lb/in^2)	274 (39,753)	168 (24,411)	134 (19,407)
	T	218	134	106

TABLE 6

COMPARISON OF COMPUTED AND MEASURED CRACK LENGTHS BASED ON THE EXPERIMENTAL COMPLIANCE EQUATION FOR THE LVDT RESULTS

a/W	% SG	0% Meas	0% LVDT	10% Meas	10% LVDT	20% Meas	20% LVDT
0.5	a_o	1.0530	1.0440	1.0387	1.0333	1.0290	1.0406
	a_f	1.1603	1.1227	1.1437	1.1148	1.1150	1.1179
	a	0.1073	0.0787	0.1050	0.0815	0.0860	0.0773
0.6	a_o	1.2301	1.2332	1.2384	1.2431	1.2461	1.2599
	a_f	1.3244	1.3024	1.3281	1.3174	1.3280	1.3394
	a	0.0943	0.0692	0.0897	0.0743	0.0819	0.0795
0.7	a_o	1.4464	1.4431	1.4468	1.4470	1.4391	1.4524
	a_f	1.5467	1.5161	1.5291	1.5087	1.5083	1.5138
	a	0.1003	0.0730	0.0823	0.0617	0.0692	0.0614
0.8	a_o	1.7096	1.7101	1.6249	1.6177	1.6232	1.6245
	a_f	1.7676	1.7615	1.7063	1.6931	1.7013	1.7106
	a	0.0580	0.0514	0.0814	0.0754	0.0781	0.0861

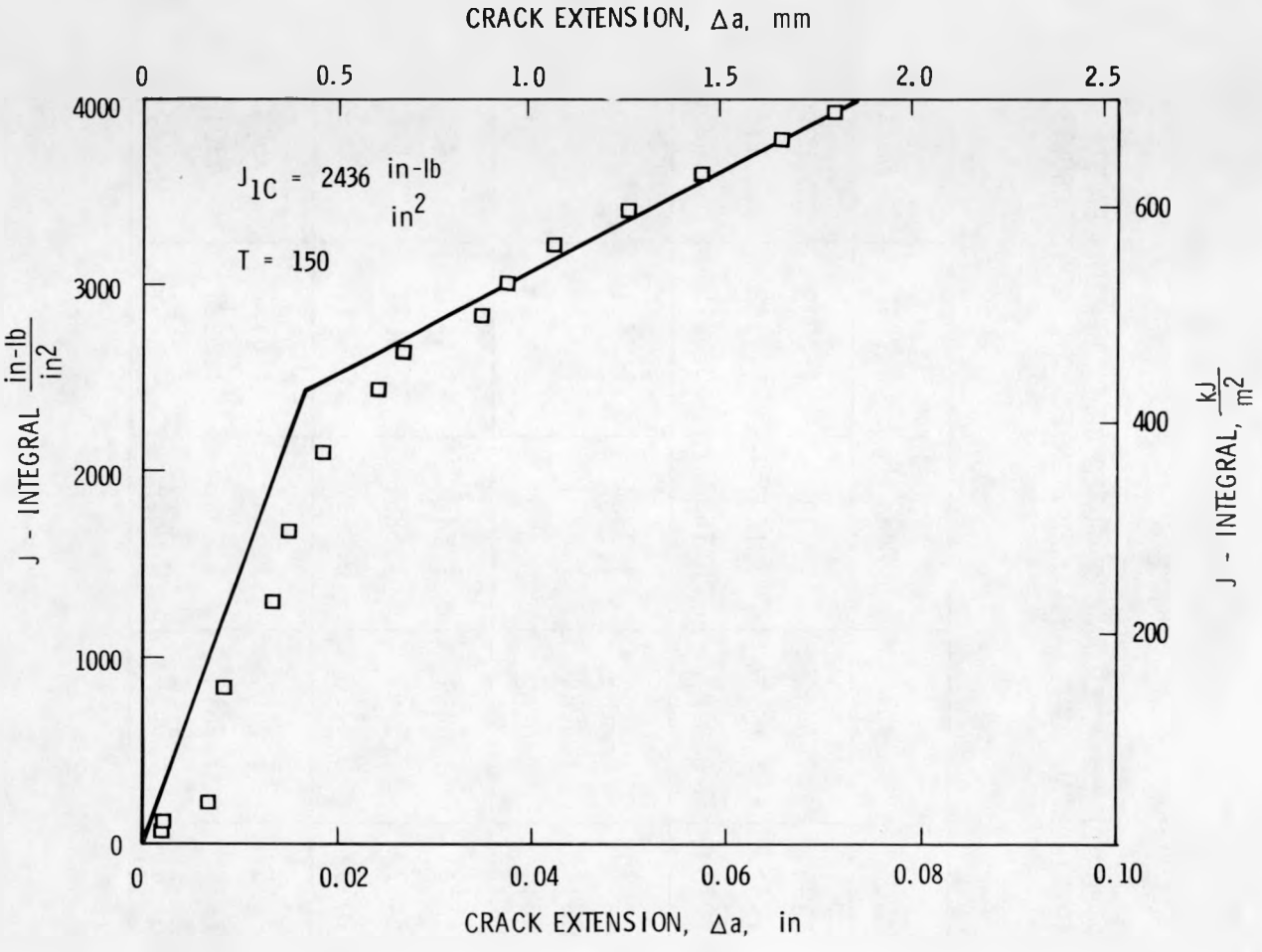

FIGURE 19. R-Curve for Specimen 02GAA1-47 (a/W = 0.5, % SG = 0) from the LVDT.

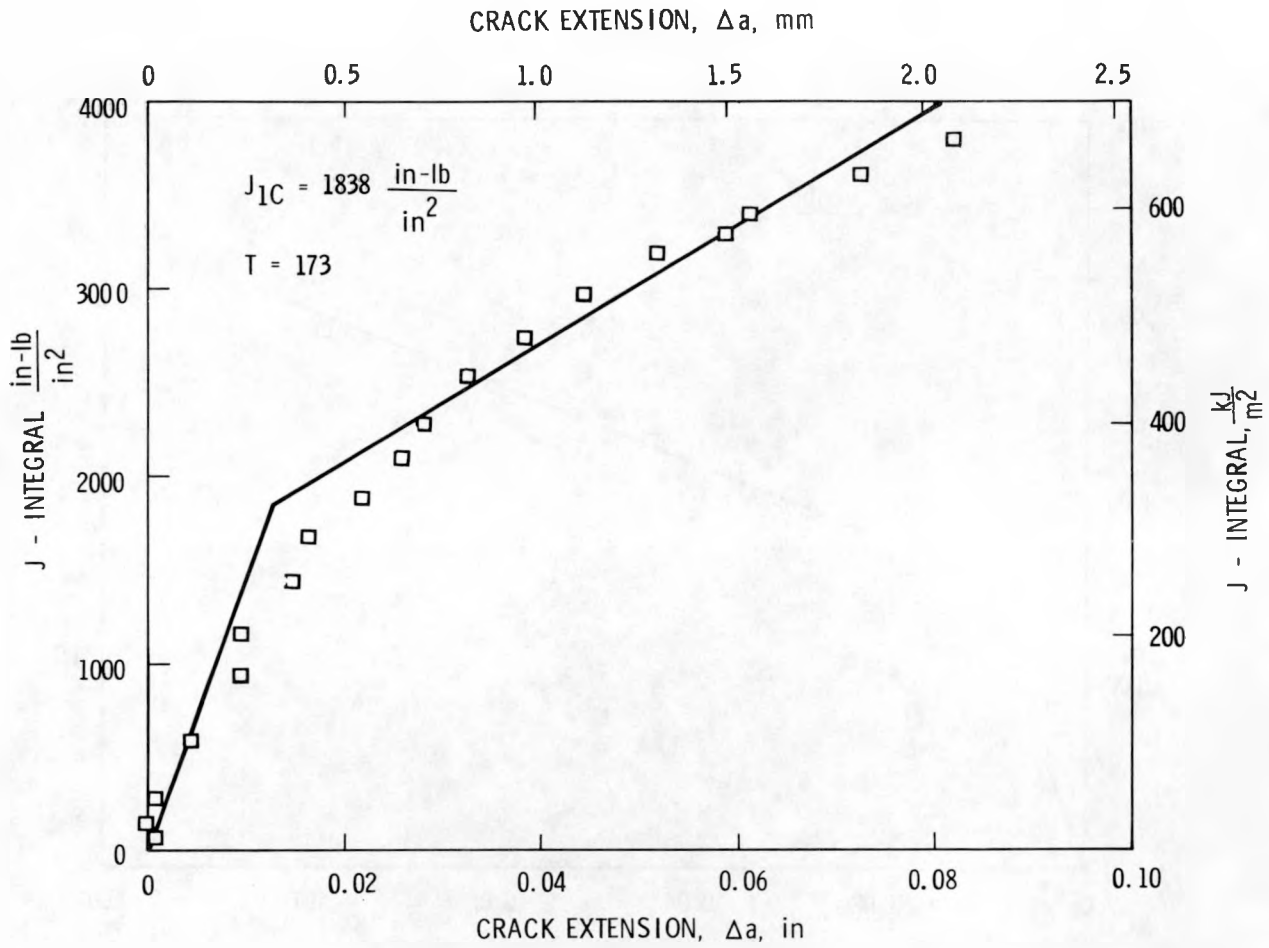

FIGURE 20. R-Curve for Specimen 02GAA1-34 (a/W = 0.5, % SG = 10) from the LVDT.

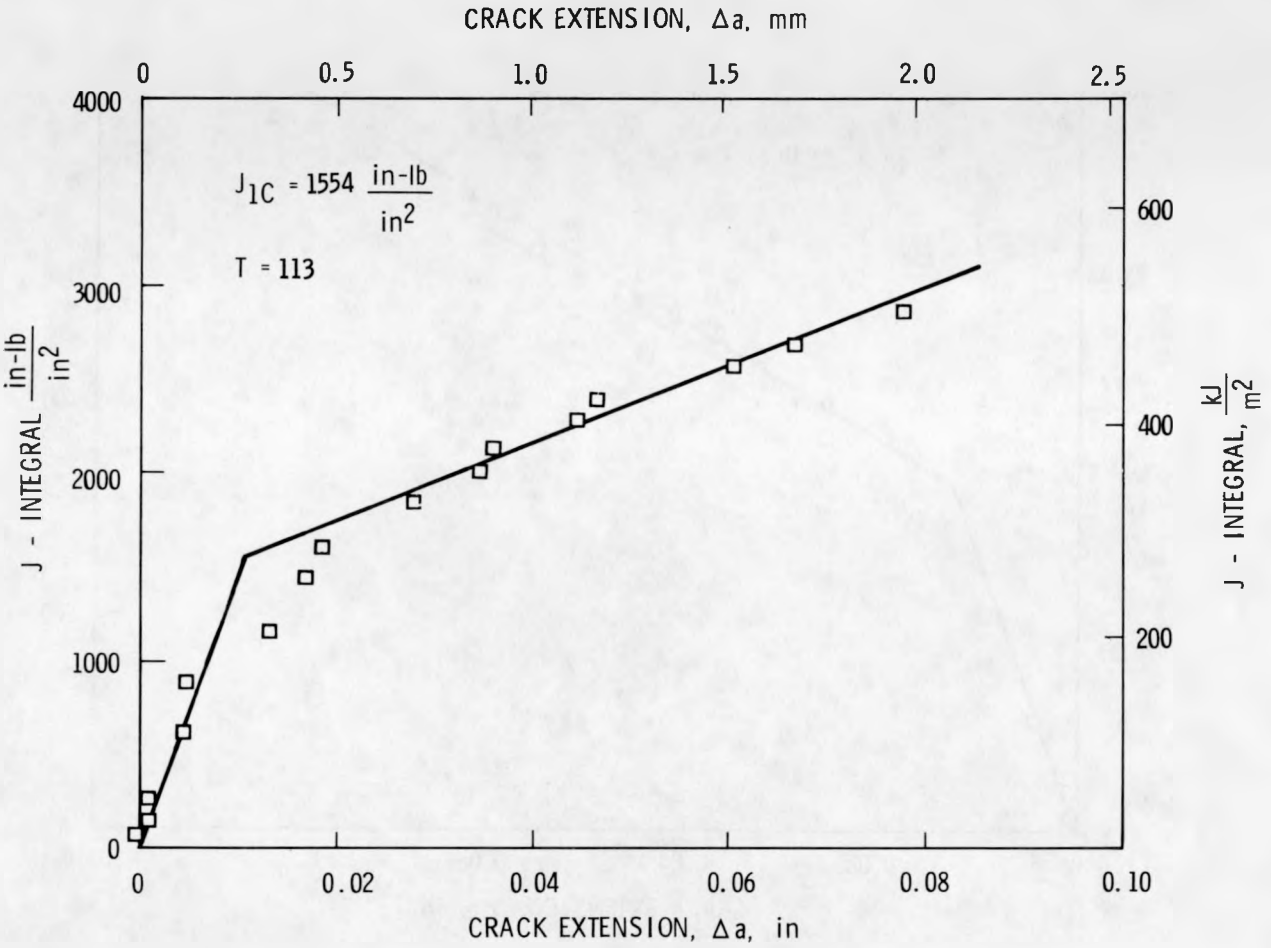

FIGURE 21. R-Curve for Specimen 02GAA1-36 (a/W = 0.5, % SG = 20) from the LVDT.

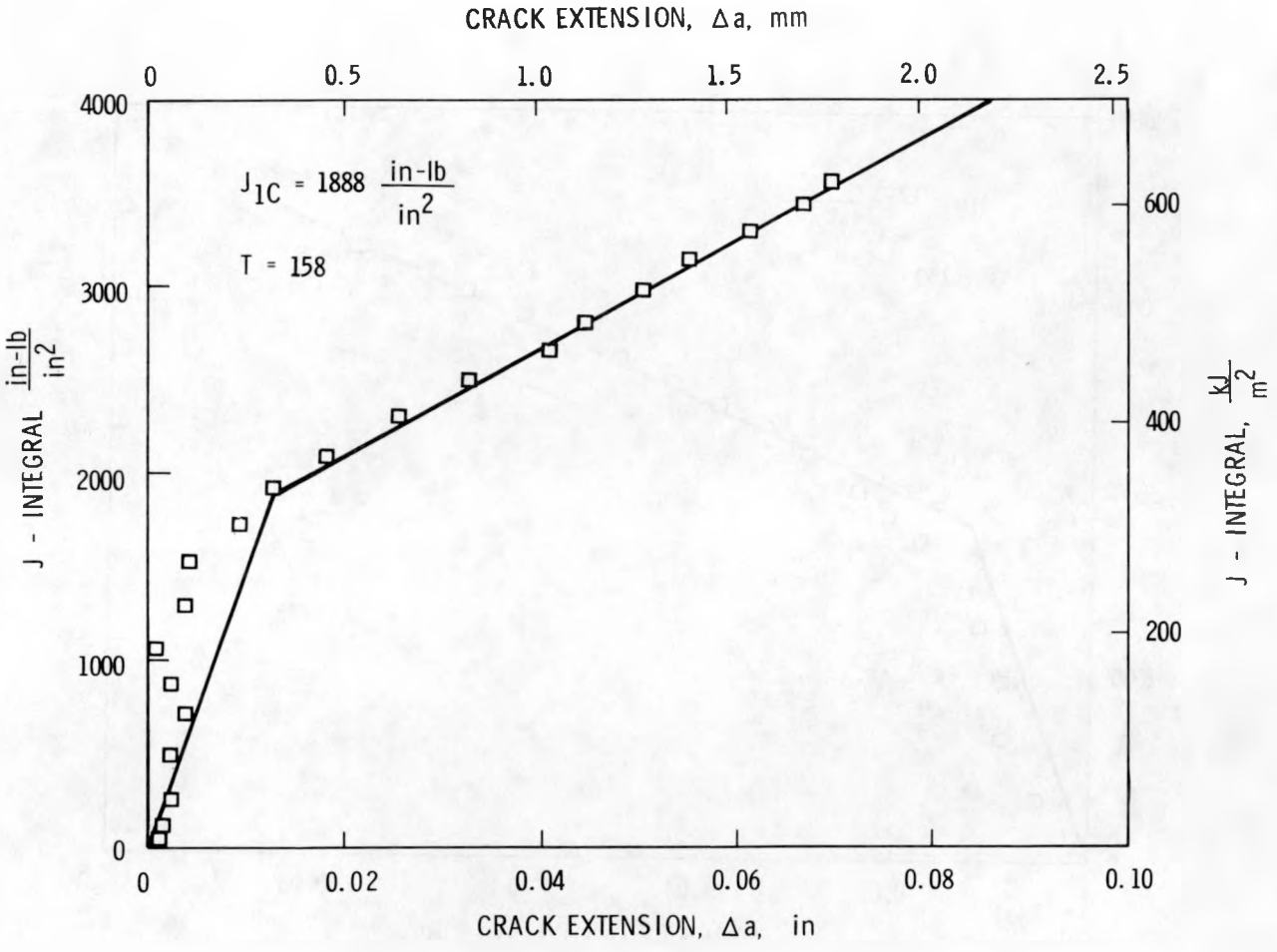

FIGURE 22. R-Curve for Specimen 02GAA1-143 (a/W = 0.6, % SG = 0) from the LVDT.

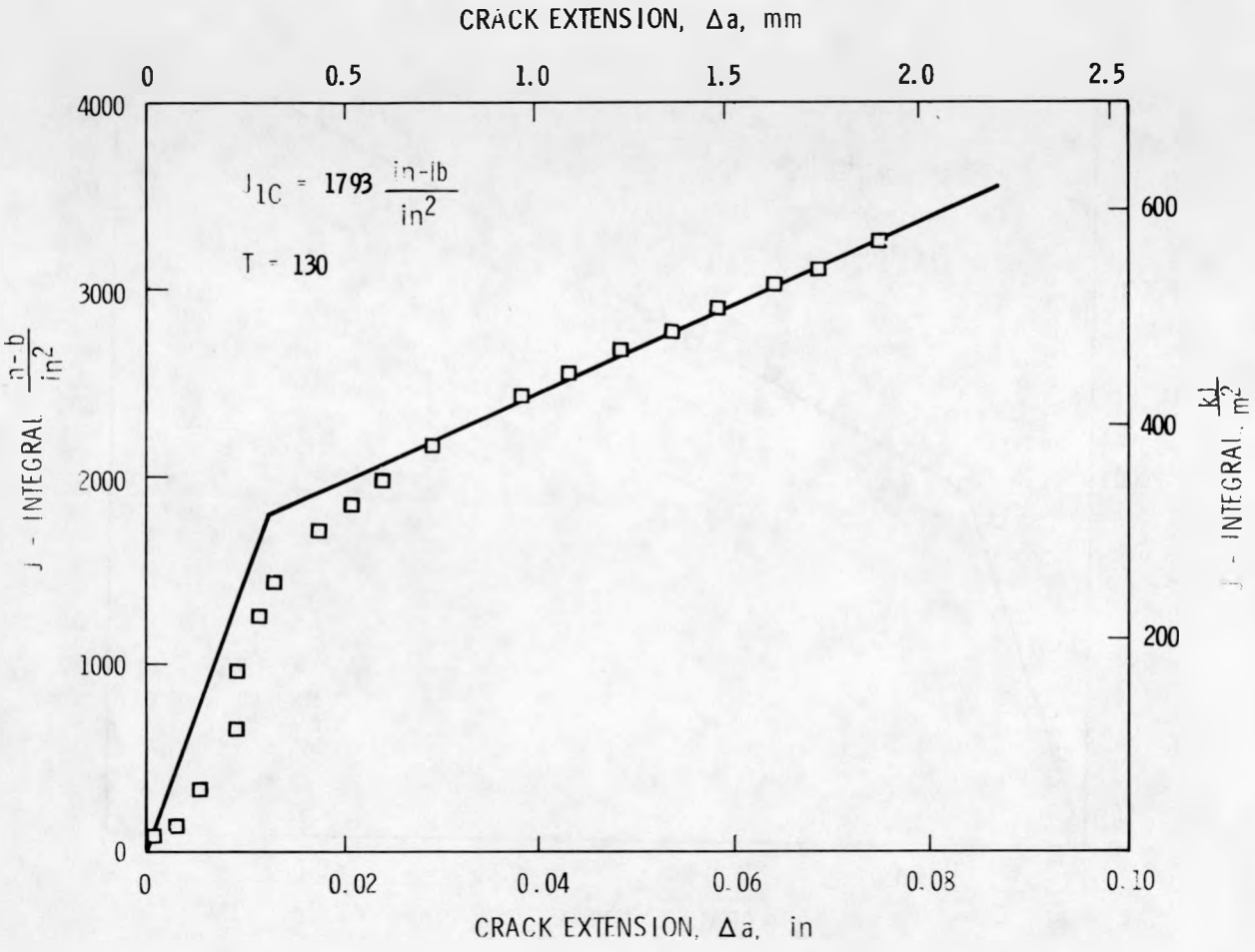

FIGURE 23. R-Curve for Specimen 02GAA1-38 (a/W = 0.6, % SG = 10) from the LVDT.

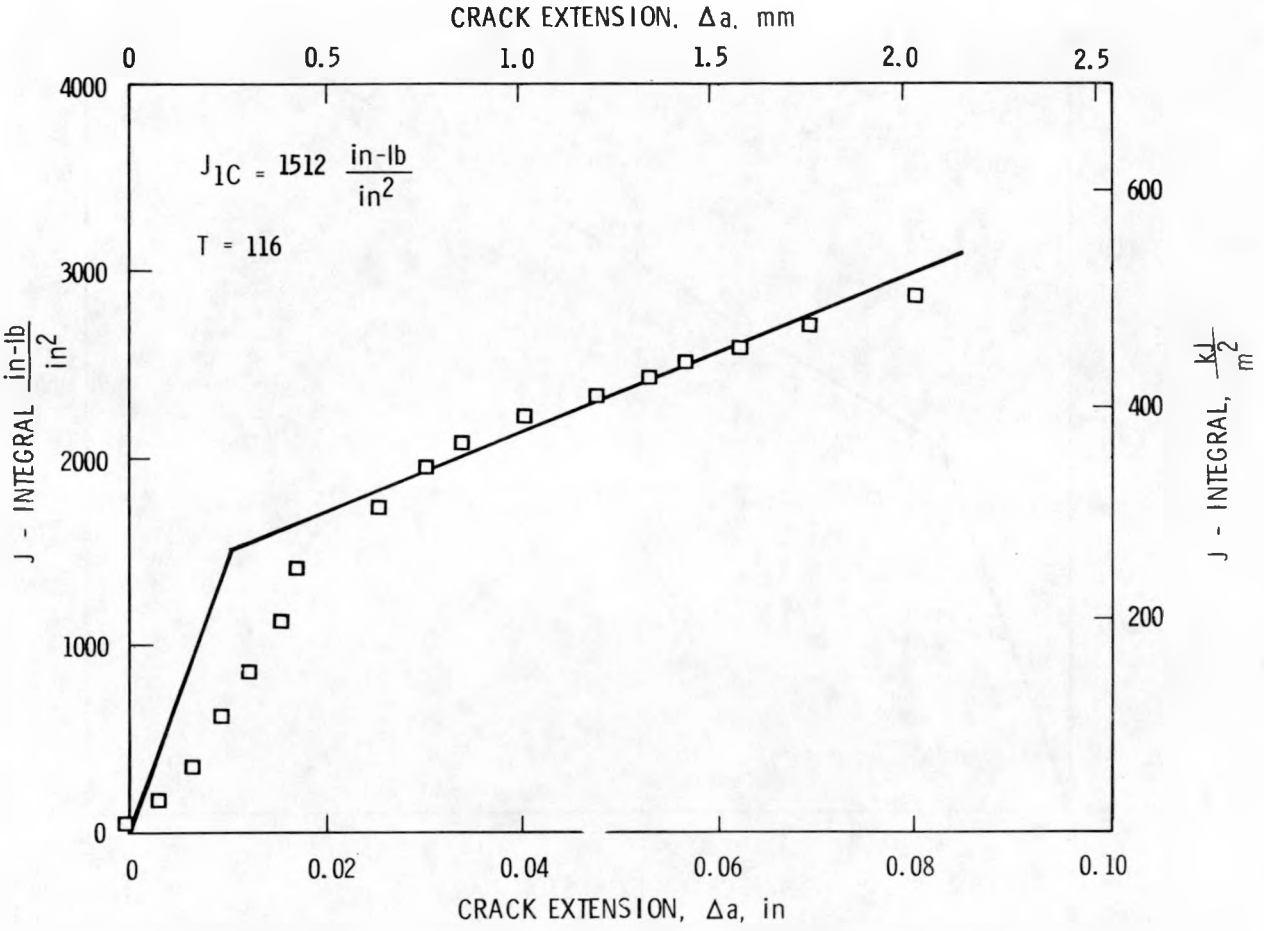

FIGURE 24. R-Curve for Specimen 02GAA1-40 (a/W = 0.6, % SG = 20) from the LVDT.

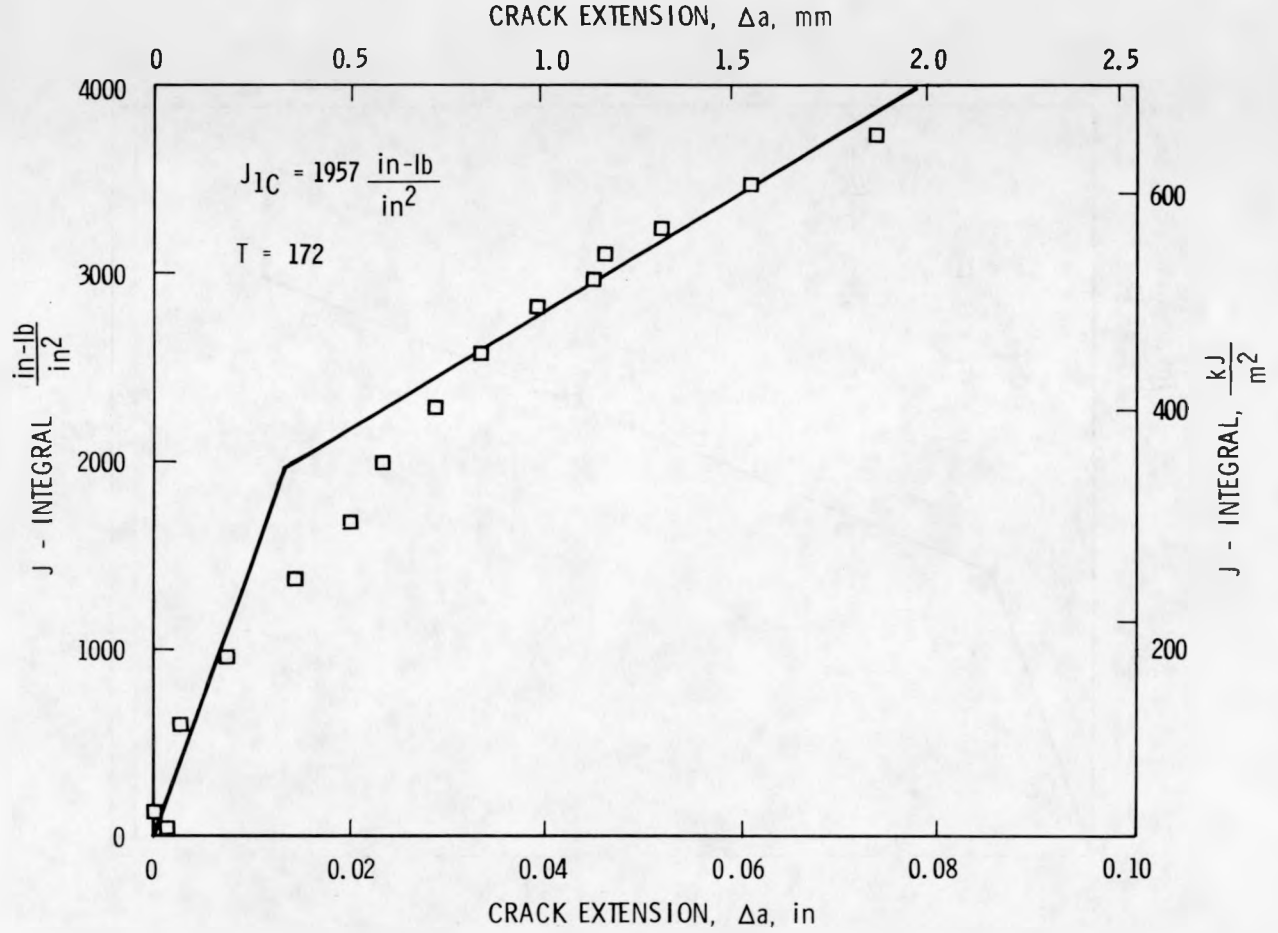

FIGURE 25. R-Curve for Specimen 02GA603 (a/W = 0.7, % SG = 0) from the LVDT.

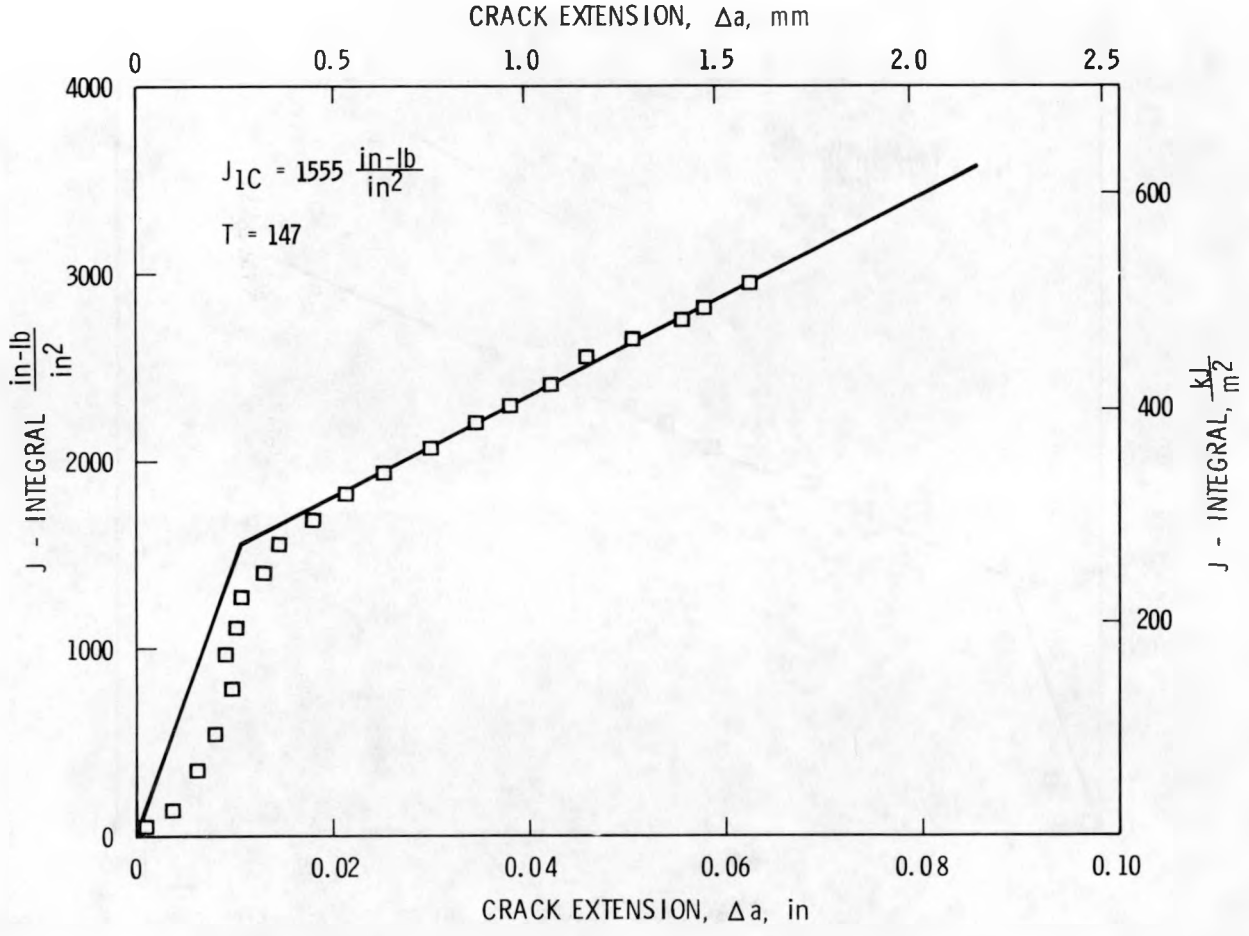

FIGURE 26. R-Curve for Specimen 02GAA1-41 (a/W = 0.7, % SG = 10) from the LVDT.

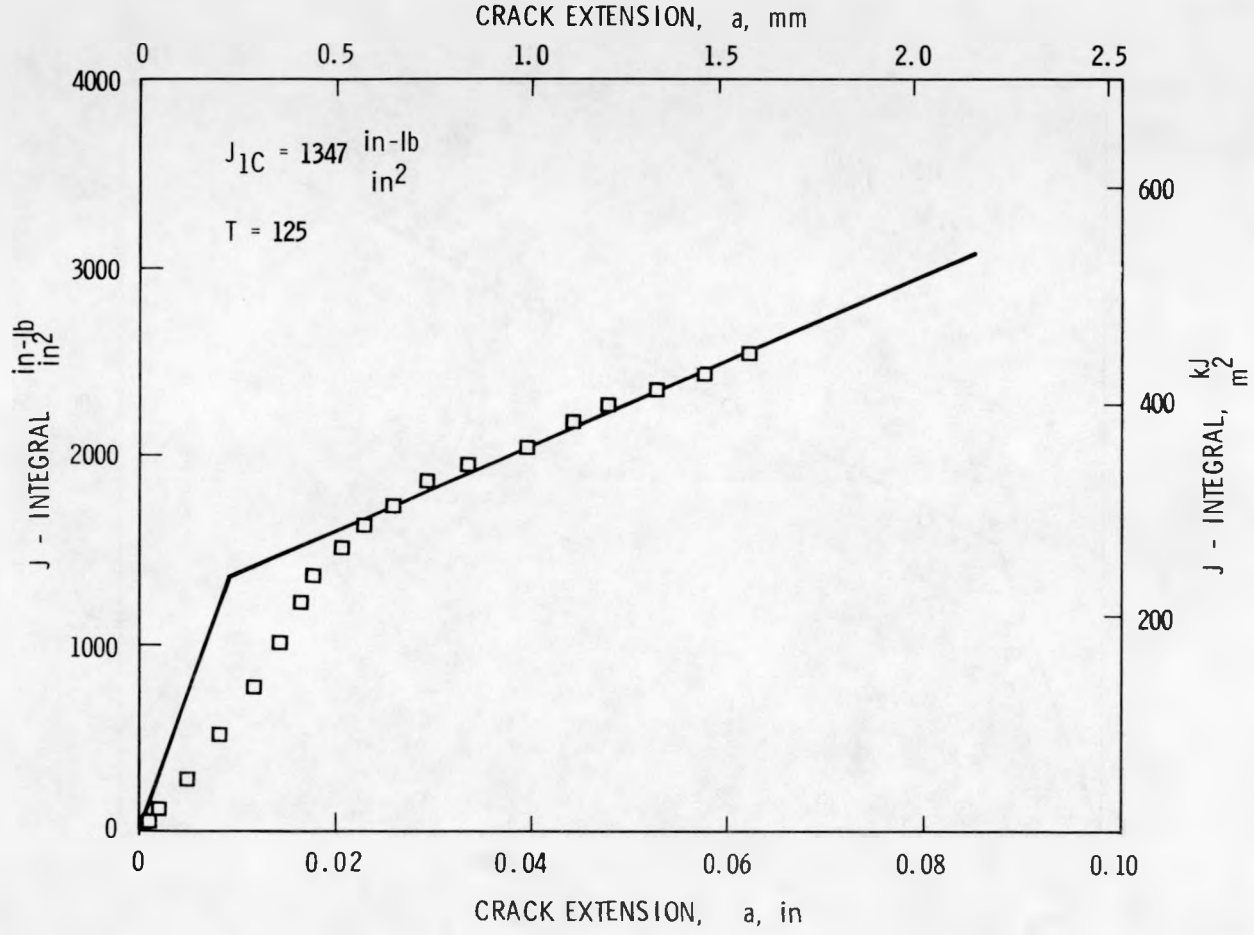

FIGURE 27. R-Curve for Specimen 02GAA1-43 (a/W = 0.7, % SG = 20) from the LVDT.

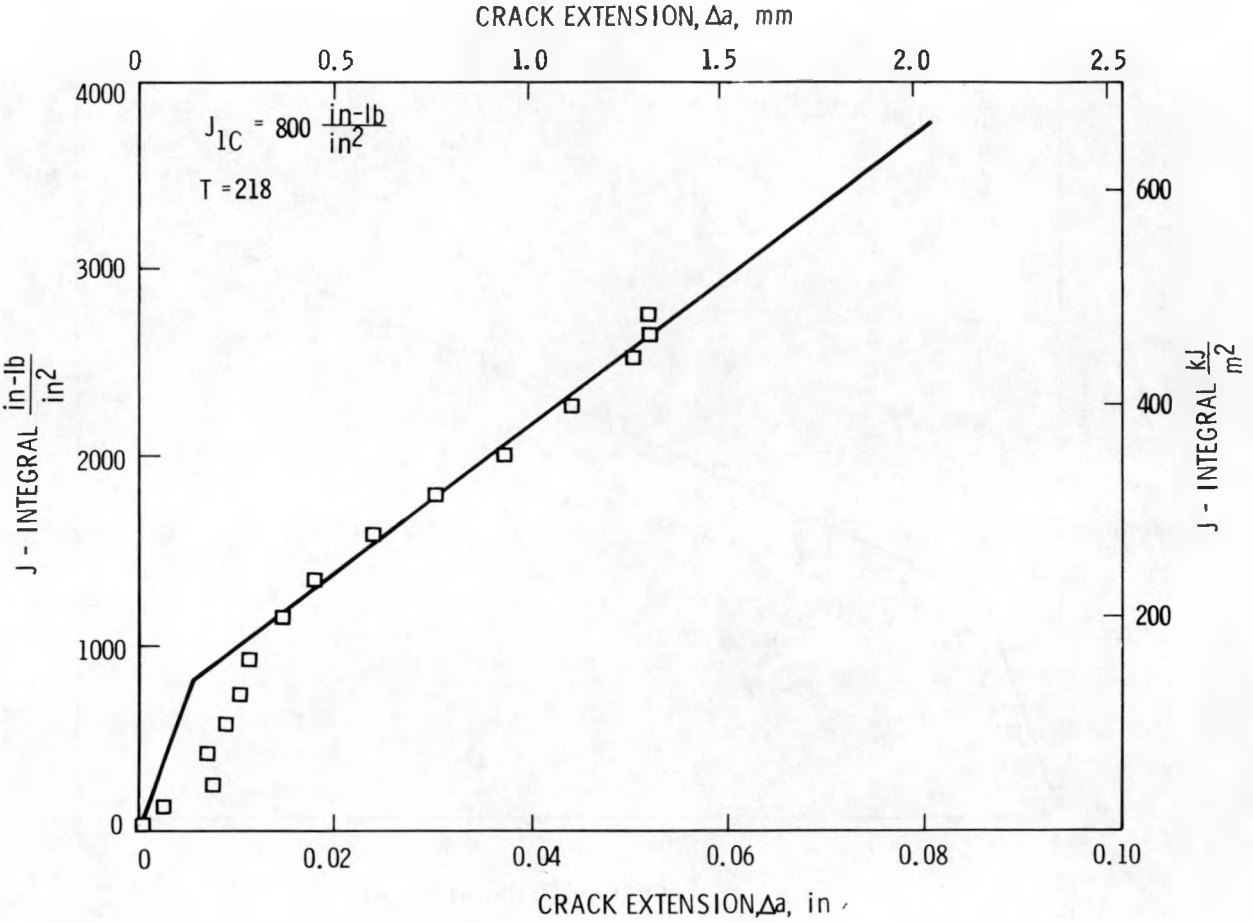

FIGURE 28. R-Curve for Specimen 02GAA1-28 (a/W = 0.8, % SG = 0) from the LVDT.

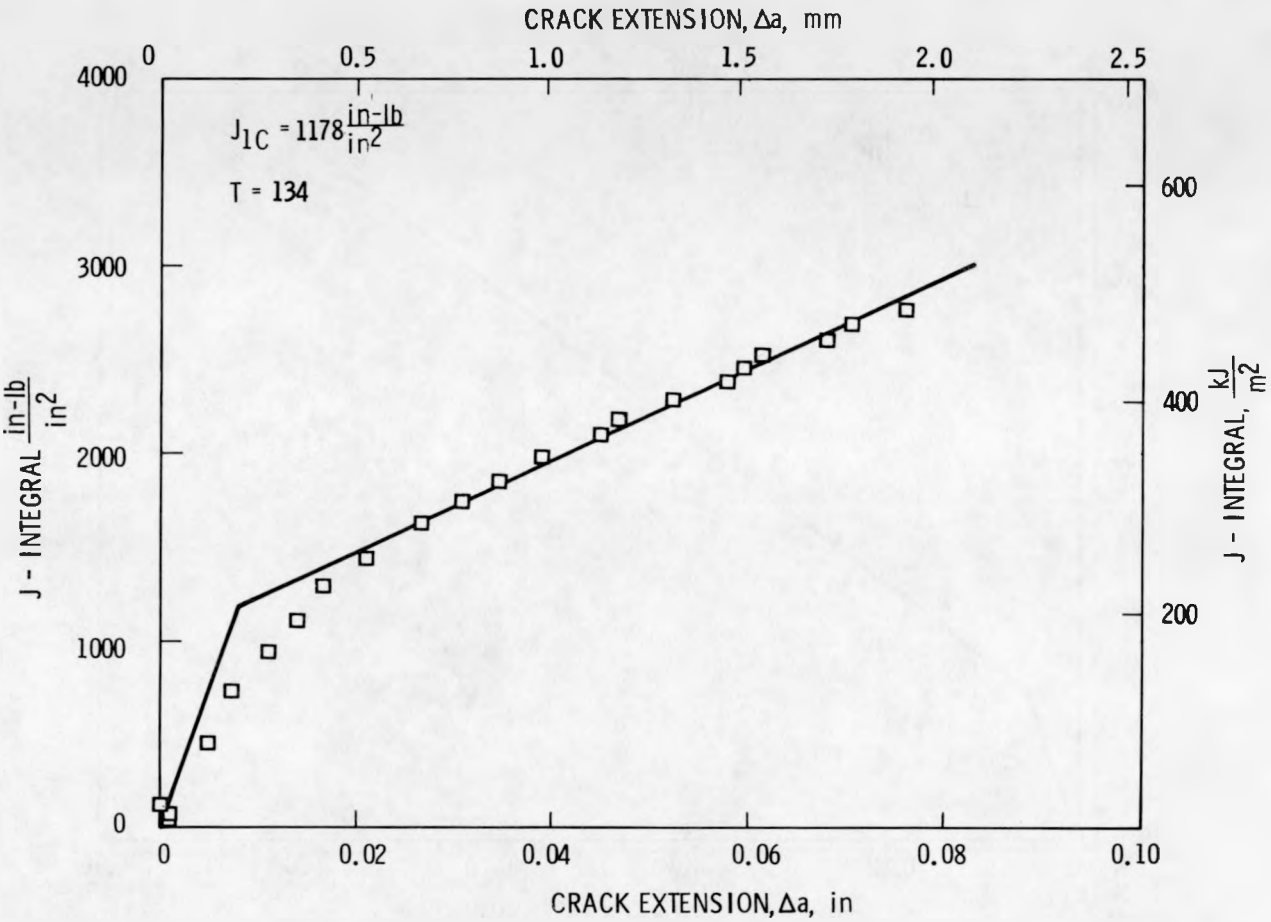

FIGURE 29. R-Curve for Specimen 02GAA1-45 (a/W = 0.8, % SG = 10) from the LVDT.

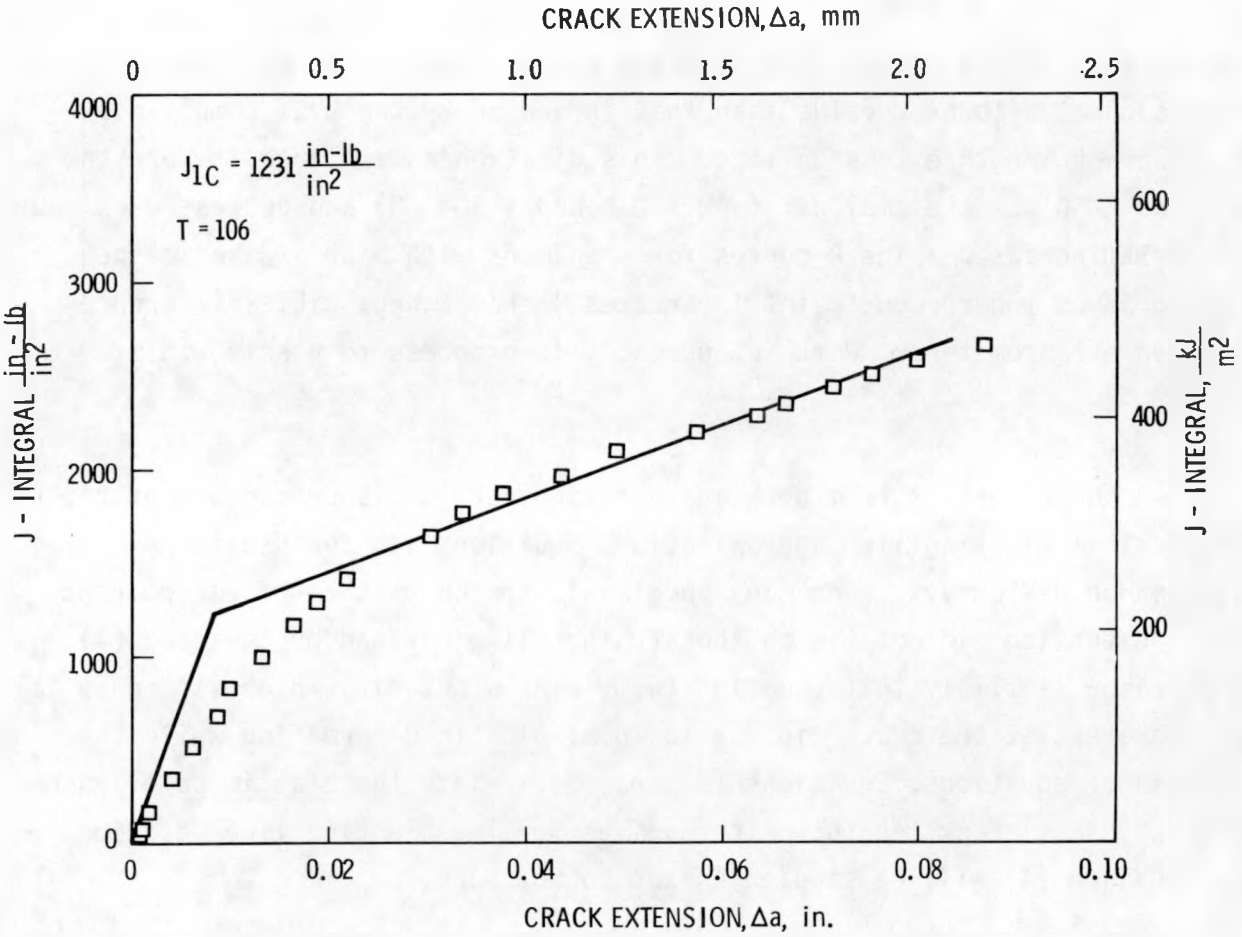

FIGURE 30. R-Curve for Specimen 02GAA1-46 (a/W = 0.8, % SG = 20) from the LVDT.

compliance equation, Equation (6), yields comparable results to the clip gage mounted at the load line on the crack plane and modeled by the Saxena-Hudak equation, Equation (3). Both systems measure initial compliance and compute initial crack length reasonably well; the respective compliance equations did not account for crack front tunneling. There are, however, some differences in the R-curves from the clip gage and LVDT extensometers. While they measure comparable initial crack lengths, the clip gage compliance-based crack length extension line often seems to indicate the onset of crack extension at a lower J value than that indicated by the LVDT compliance-based crack length extension line. This difference was largest where the a/W and % SG was the smallest (a/W = 0.5 and % SG = 0) and decreased as a/W and % SG increased. The R-curves for specimens with high a/W and deeper side grooves (where constraint is greatest) show a negligible difference between extensometers. Work is currently in progress to resolve this matter.

The J-R curve results from both analyses indicate the shortcomings of the theoretical blunting line approximation, Equation (4), for use in unloading compliance J-R curves. For many specimens, the compliance-based apparent crack extension did not lie on the straight line defined by Equation (4). The reason is simply that Equation (4) yields a quantity which is a physical displacement at the crack tip due to local plastic deformation while the compliance equations, Equations (3) and (5), relate the elastic compliance with physical crack length. Alternatives for the blunting line described by Equation (4) will be studied in subsequent work.

C. RECOMMENDED FUTURE WORK

It is recommended that multiple-specimen heat tint R-curves be developed for a number of specimen dimensions contained in the present test matrix. In doing this, the directly measured crack extension characteristics can be correlated with the unloading compliance behavior of the two extensometers.

It is also desirable to develop an alternative to the theoretical blunting line, Equation (4), which actually fits the unloading compliance data during blunting. A linear regression line through these data points may serve quite well.

V. REFERENCES

1. J. R. Rice, "A Path Independent Integral and the Approximate Analysis of Strain Concentration by Notches and Cracks," ASME, Journal of Applied Mechanics 35, pp. 379-386, 1968.

2. J. R. Rice, "Mathematical Analysis in the Mechanics of Fracture," in Fracture, H. Liebowitz, Ed., Vol. 2, Academic Press, New York, NY, pp. 191-311, 1968.

3. J. A. Begley and J. D. Landes, "The J-Integral as a Fracture Criterion," Fracture Toughness, ASTM STP 514, pp. 1-23, 1972.

4. J. D. Landes and J. A. Begley, "The Effect of Specimen Geometry on J_{Ic} at Failure," Fracture Toughness, ASTM STP 514, pp. 40-69, 1974.

5. R. J. Bucci, P. C. Paris, J. D. Landes and J. R. Rice, "J-Integral Estimation Procedures," Fracture Toughness, ASTM STP 514, pp. 40-69, 1972.

6. J. R. Rice, P. C. Paris and J. G. Merkle, "Some Further Results of J-Integral Analysis and Estimates," Progress in Flaw Growth and Fracture Toughness Testing, ASTM STP 536, pp. 231-245, 1973.

7. J. D. Landes and J. A. Begley, "Test Results from J-Integral Studies--An Attempt to Establish a J_{Ic} Testing Procedure," Fracture Analysis, ASTM STP 560, pp. 170-186, 1974.

8. J. A. Begley (on behalf of ASTM Task Group E-24:01:09), "Recommended Practices for the Determination of the J_{Ic} Point from the J Versus Δa R-Curve," presented at the American Society for Testing and Materials E-24 Committee Meetings, Philadelphia, PA, October 7, 1976.

9. G. A. Clarke, W. R. Andrews, J. A. Begley, J. K. Donald, G. T. Embley, J. D. Landes, D. E. McCabe and J. H. Underwood, "A Procedure for the Determination of Ductile Fracture Toughness Values Using J Integral Techniques," Journal of Testing and Evaluation 7, No. 1, pp. 49-56, January 1979.

10. G. A. Clarke, W. A. Andrews, P. C. Paris and D. W. Schmidt, "Single Specimen Tests for J_{Ic} Determination," Mechanics of Crack Growth, ASTM STP 590, pp. 27-42, 1976.

11. B. Marandet and G. Sanz, "Experimental Verification of the J_{Ic} and Equivalent Energy Methods for the Evaluation of the Fracture Toughness of Steels," Flaw Growth and Fracture, ASTM STP 631, pp. 462-476, 1977.

12. K. Markstrom, "Experimental Determination of J_c Data Using Different Types of Specimens," Publication No. 199, Department of Strength of Materials and Solid Mechanics, The Royal Institute of Technology, Stockholm, Sweden, 1975.

13. S. Taira and K. Tanaka, "Thickness Effect of Notched Metal Sheets on Deformation and Fracture Under Tension," Engineering Fracture Mechanics 11, pp. 231-249, 1979.

14. C. E. Childress, Fabrication History of the First Two 12-Inch Thick ASTM A533 Grade B, Class 1 Steel Plates of the Heavy Section Steel Technology Program, Documentary Report 1, ORNL-4313, Oak Ridge National Laboratory, Oak Ridge, TN, February 1969.

15. J. A. Williams, The Irradiation and Temperature Dependence of Tensile and Fracture Properties of ASTM A533, Grade B, Class 1 Steel Plate and Weldment, HEDL-TME 73-75, HSSTP Tech. Rept. 31, Hanford Engineering Development Laboratory, Richland, WA, August 1973.

16. J. M. Steichen and J. A. Williams, High Strain Rate Tensile Properties of Irradiated ASTM A533-B Pressure Vessel Steel, HEDL-TME 73-74, HSSTP Tech. Rept. 32, Hanford Engineering Development Laboratory, Richland, WA, July 1973.

17. W. J. Stelzman and R. G. Berggren, Radiation Strengthening and Embrittlement in Heavy Section Steel Plates and Welds, ORNL-4871, Oak Ridge National Laboratory, Oak Ridge, TN, June 1973.

18. W. J. Mills, L. A. James and J. A. Williams, "A Technique for Measuring Load-Line Displacements of Compact Ductile Fracture Toughness Specimens at Elevated Temperatures," Journal of Testing and Evaluation 5, No. 6, pp. 446-451, November 1977.

19. J. G. Merkle and H. T. Corten, "A J Integral Analysis for the Compact Specimen, Considering Axial Force as Well as Bending Effects," Journal of Pressure Vessel Technology, American Society of Mechanical Engineers, 1974.

20. A. Saxena and S. J. Hudak, Jr., "Review and Extension of Compliance Information for Common Crack Growth Specimens," Westinghouse Scientific Paper No. 77-9E7-AFCGR-P1, May 1977.

21. P. C. Paris, H. Tada, A. Zahoor and H. Ernst, "Instability of the Tearing Mode of Elastic-Plastic Crack Growth," Elastic-Plastic Fracture, ASTM STP 668, pp. 5-36, 1979.

DISTRIBUTION

R5 (265)

RF (168)

Nuclear Regulatory Commission
Washington, DC 20555

CZ Serpan, RSR

DOE/Oak Ridge Operations Office
P. O. Box E
Oak Ridge, TN 37830

Office of Assistant Manager

DOE/FFTFPO (5)
P. O. Box 550
Richland, WA 99352

Director (5)

DOE/TIC (2)
P. O. Box 62
Oak Ridge, TN 37830

Director (2)

Oak Ridge National Laboratory (48)
P. O. Box X
Oak Ridge, TN 37830

RG Berggren
SE Bolt
RH Bryan
JW Bryson
DA Canonico
RD Cheverton
JM Corum
WB Cottrell
JR Dougan
WL Greenstreet
RC Gwaltney
PP Holz
SK Iskander
KK Klindt
M. Levenson
JG Merkle
CA Mills
SE Moore
RF Mynatt
DJ Naus
GC Robinson
GM Slaughter
JE Smith
WJ Stelzman
HE Trammell
GD Whitman (14)
Patent Office
Central Research Library (2)
Document Reference Section
Laboratory Records Dept. (4)
Laboratory Records (Record Copy)

Hanford Engineering Development Laboratory (50)
P. O. Box 1970
Richland, WA 99352
Attn: Supervisor, Document Processing W/C-123

RG Bentley	W/A-40	MD Jones	W/A-40
LD Blackburn	W/A-40	RL Knecht	W/A-40
KW Carlson	W/A-40	GC Massie	W/A-40
DJ Criswell	W/A-40	WN McElroy	W/C-39
JM Dahlke	W/C-115	DA Mervyn	W/A-58
EA Evans	W/JAD-6	WJ Mills	W/A-40
GL Guthrie	W/C-39	JL Straalsund	W/A-57
BR Hayward	W/A-62	AL Ward	W/JAD-7
GW Hollenberg	W/A-59	JA Williams (13)	W/A-40
JJ Holmes	W/A-58	MJ Wilson	W/C-115
WL Hu	W/A-58	GL Wire	W/A-58
CW Hunter	W/A-53	HH Yoshikawa	W/A-62
LA James	W/A-40	Central Files (10)	W/C-110
		Publ Services (2)	W/C-115
		Contract Admin SW Berglin	W/A-21

RC FORM 335 (77)

U.S. NUCLEAR REGULATORY COMMISSION

BIBLIOGRAPHIC DATA SHEET

1. REPORT NUMBER *(Assigned by DDC)*
NUREG/CR- 1171

TITLE AND SUBTITLE *(Add Volume No., if appropriate)*
The Effect of Crack Length and Side Grooves on the Ductile Fracture Toughness Properties of ASTM A533 Steel

2. *(Leave blank)*

3. RECIPIENT'S ACCESSION NO.

AUTHOR(S)
K. W. Carlson, J. A. Williams

5. DATE REPORT COMPLETED
MONTH | YEAR

PERFORMING ORGANIZATION NAME AND MAILING ADDRESS *(Include Zip Code)*
Hanford Engineering Development Laboratory
P. O. Box 1970
Richland, WA 99352

DATE REPORT ISSUED
MONTH | YEAR
January 1980

6. *(Leave blank)*
February 1980

8. *(Leave blank)*

SPONSORING ORGANIZATION NAME AND MAILING ADDRESS *(Include Zip Code)*
Office of Nuclear Regulatory Research
U. S. Nuclear Regulatory Commission
Washington, D. C. 20555

10. PROJECT/TASK/WORK UNIT NO.

11. CONTRACT NO.
NRC FIN No. B0119

TYPE OF REPORT

PERIOD COVERED *(Inclusive dates)*

SUPPLEMENTARY NOTES

14. *(Leave blank)*

ABSTRACT *(200 words or less)*

The ductile fracture toughness, J_{IC}, and tearing modulus, T, of ASTM A533, Grade B, Class 1 steel were evaluated by the unloading compliance method for determining J-R curves. These properties were measured for a matrix of IT specimens in which the relative crack length, a/W, and the depth of side grooving were systematically varied to determine their individual effects. In addition, the applicability of an LVDT extensometer system was investigated for use in the unloading compliance method for J-R curve determination.

KEY WORDS AND DOCUMENT ANALYSIS

17a. DESCRIPTORS

b. IDENTIFIERS/OPEN-ENDED TERMS

AVAILABILITY STATEMENT
Unlimited

19. SECURITY CLASS *(This report)*
Unclassified

21. NO. OF PAGES

20. SECURITY CLASS *(This page)*
Unclassified

22. PRICE
S